

## DISCONTINUOUS GALERKIN DISCRETIZATIONS OF OPTIMIZED SCHWARZ METHODS FOR SOLVING THE TIME-HARMONIC MAXWELL'S EQUATIONS\*

MOHAMED EL BOUAJAJI<sup>†</sup>, VICTORITA DOLEAN<sup>‡</sup>, MARTIN J. GANDER<sup>§</sup>, STÉPHANE LANTERI<sup>†</sup>,  
AND RONAN PERRUSSEL<sup>¶</sup>

**Abstract.** We show in this paper how to properly discretize optimized Schwarz methods for the time-harmonic Maxwell's equations in two and three spatial dimensions using a discontinuous Galerkin (DG) method. Due to the multiple traces between elements in the DG formulation, it is not clear a priori how the more sophisticated transmission conditions in optimized Schwarz methods should be discretized, and the most natural approach, at convergence of the Schwarz method, does not lead to the monodomain DG solution, which implies that for such discretizations, the DG error estimates do not hold when the Schwarz method has converged. We present here a consistent discretization of the transmission conditions in the framework of a DG weak formulation, for which we prove that the multidomain and monodomain solutions for the Maxwell's equations are the same. We illustrate our results with several numerical experiments of propagation problems in homogeneous and heterogeneous media.

**Key words.** computational electromagnetism, time-harmonic Maxwell's equations, Discontinuous Galerkin method, optimized Schwarz methods, transmission conditions.

**AMS subject classifications.** 65M55, 65F10, 65N22

**1. Introduction.** Discontinuous Galerkin (DG) methods have received a lot of attention over the last decade since they combine the best of both finite-element and finite-volume methods. The approximation of each field is done locally at the level of each mesh element by using a local basis of functions, and the discontinuity between neighboring elements is treated using a finite-volume flux. A richer representation of the solution is given at the price of increasing the total number of degrees of freedom as a result of the decoupling of elements. The literature on these methods applied to different types of equations is rich, and we will focus on contributions concerning Maxwell's equations. A complete historical introduction with a large panel of references can be found in the milestone book on DG methods by Hesthaven and Warburton [28].

Theoretical results on DG methods applied to the time-harmonic Maxwell's equations have been obtained by several authors. Most of these use the second-order formulation of the Maxwell's equations. An alternative is to use the first-order formulation as in [25, 26, 27] based on the theory of Friedrichs systems. In a large part of the literature on time-harmonic problems, a mixed formulation is used (see [30, 35]), but DG methods for the non-mixed formulation, like interior penalty techniques [5, 29] and local discontinuous Galerkin methods [5], have also been studied. A numerical convergence study of discontinuous Galerkin methods based on centered and upwind fluxes and nodal polynomial interpolation applied to the first-order time-harmonic Maxwell system in the two-dimensional case can be found in [10].

Like for all other discretizations of the time-harmonic Maxwell's equations, it is also difficult to solve linear systems obtained by DG discretizations with iterative methods. Due to the indefinite nature of the problems, classical iterative solvers fail as in the Helmholtz

\*Received September 10, 2014. Accepted August 12, 2015. Published online on November 3, 2015. Recommended by U. Langer.

<sup>†</sup>INRIA Sophia Antipolis-Méditerranée, 06902 Sophia Antipolis Cedex, France  
({Mohamed.El\_bouajaji, Stephane.Lanteri}@inria.fr).

<sup>‡</sup>Université de Nice Sophia-Antipolis, Laboratoire J.-A. Dieudonné, Nice, France (dolean@unice.fr).

<sup>§</sup>Section de Mathématiques, Université de Genève, CP 64, 1211 Genève, Switzerland  
(Martin.Gander@math.unige.ch).

<sup>¶</sup>CNRS, Université de Toulouse, Laboratoire plasma et conversion d'énergie, 31071 Toulouse Cedex 7, France  
(perrussel@laplace.univ-tlse.fr).

case [18]. Després defined in [8] a first provably convergent domain decomposition algorithm for the Helmholtz equation. This algorithm was extended to Maxwell's equations in [9]. Even better transmission conditions were proposed in [6, 7, 23] based on optimized Schwarz theory [19, 20] with an application to the second-order Maxwell system in [1]. An entire hierarchy of optimized Schwarz methods for the first-order Maxwell's equations can be found in [11] with complete asymptotic results for the optimization. DG discretizations of optimized Schwarz methods for time-harmonic Maxwell's equations were proposed first in [15]. In the short proceedings paper [17], the authors proposed a different DG discretization of the transmission conditions for the TM formulation of Maxwell's equation in two spatial dimensions and stated an equivalence theorem of the decomposed DG solution with the monodomain DG solution without a proof. The purpose of our manuscript is to prove this theorem and also to present a consistent DG discretization for Maxwell's equations in three spatial dimensions together with an equivalence theorem which is more involved to prove than in the two-dimensional case. Classical finite-element based non-overlapping and non-conforming domain decomposition methods for the computation of multiscale electromagnetic radiation and scattering problems can be found in [31, 32, 33, 34, 36, 37]. They do not need any special treatment for the discretization of the optimized transmission conditions. For DG discretizations, however, even for the Poisson equation, the discretization of transmission conditions needs to be done with care [22, 24], and classical block Jacobi methods are not equivalent to classical Schwarz methods for DG discretizations [21].

This paper is organized as follows: in Section 2 we present the three-dimensional time-harmonic Maxwell's equations as a first-order system and introduce the notation for what follows. In Section 3 we state the classical and optimized Schwarz algorithm at the continuous level for the first-order Maxwell system in 3D. In Section 4, we introduce a weak formulation for the first-order system and use a DG approximation to obtain discrete subdomain problems. We then show that while the DG discretization of the classical Schwarz method is very natural, the optimized transmission conditions are more tricky to discretize, and we present for the three-dimensional Maxwell's equations a consistent discretization of the transmission conditions, for which we prove that the monodomain and multidomain formulations are equivalent. Next we also prove the equivalence result for the two-dimensional TM formulation announced in the proceedings paper [17]. We finally provide in Section 5 results of several numerical experiments for both homogeneous and heterogeneous propagation problems to illustrate the performance of the optimized Schwarz methods as solvers for DG-discretized Maxwell's equations. Section 6 contains a brief conclusion.

**2. The time-harmonic Maxwell system.** The time-harmonic Maxwell's equations in a homogeneous medium are given by

$$(2.1) \quad i\omega\varepsilon\mathbf{E} - \operatorname{curl} \mathbf{H} + \sigma\mathbf{E} = \mathbf{0}, \quad i\omega\mu\mathbf{H} + \operatorname{curl} \mathbf{E} = \mathbf{0},$$

where the positive real parameter  $\omega$  is the pulsation of the harmonic wave,  $\sigma$  is the electric conductivity,  $\varepsilon$  is the electric permittivity,  $\mu$  is the magnetic permeability, and the unknown complex-valued vector fields  $\mathbf{E}$  and  $\mathbf{H}$  are the electric and magnetic fields. In the homogeneous case, to simplify notation, we can rewrite equation (2.1) as

$$(2.2) \quad i\tilde{\omega}\mathbf{E} - \operatorname{curl} \mathbf{H} + \tilde{\sigma}\mathbf{E} = \mathbf{0}, \quad i\tilde{\omega}\mathbf{H} + \operatorname{curl} \mathbf{E} = \mathbf{0},$$

where  $\tilde{\omega} := \omega\sqrt{\varepsilon\mu}$  and  $\tilde{\sigma} := \sigma\sqrt{\frac{\mu}{\varepsilon}}$ . Collecting the variables into one big vector  $\mathbf{W} := (\mathbf{E}, \mathbf{H})$ , we can rewrite (2.2) as a first-order system,

$$G_0\mathbf{W} + G_x\partial_x\mathbf{W} + G_y\partial_y\mathbf{W} + G_z\partial_z\mathbf{W} = \mathbf{0},$$

where

$$G_0 := \begin{bmatrix} (\tilde{\sigma} + i\tilde{\omega})\mathbb{I}_{3 \times 3} & 0_{3 \times 3} \\ 0_{3 \times 3} & i\tilde{\omega}\mathbb{I}_{3 \times 3} \end{bmatrix},$$

and

$$G_x := \begin{bmatrix} 0_{3 \times 3} & N_x \\ N_x^T & 0_{3 \times 3} \end{bmatrix}, \quad G_y := \begin{bmatrix} 0_{3 \times 3} & N_y \\ N_y^T & 0_{3 \times 3} \end{bmatrix}, \quad G_z := \begin{bmatrix} 0_{3 \times 3} & N_z \\ N_z^T & 0_{3 \times 3} \end{bmatrix},$$

with

$$N_x := \begin{bmatrix} 0 & 0 & 0 \\ 0 & 0 & 1 \\ 0 & -1 & 0 \end{bmatrix}, \quad N_y := \begin{bmatrix} 0 & 0 & -1 \\ 0 & 0 & 0 \\ 1 & 0 & 0 \end{bmatrix}, \quad N_z := \begin{bmatrix} 0 & 1 & 0 \\ -1 & 0 & 0 \\ 0 & 0 & 0 \end{bmatrix}.$$

For a general vector  $\mathbf{n} = (n_x, n_y, n_z)$ , we can define the matrices

$$G_{\mathbf{n}} := \begin{bmatrix} 0_{3 \times 3} & N_{\mathbf{n}} \\ N_{\mathbf{n}}^T & 0_{3 \times 3} \end{bmatrix} \quad \text{and} \quad N_{\mathbf{n}} := \begin{bmatrix} 0 & n_z & -n_y \\ -n_z & 0 & n_x \\ n_y & -n_x & 0 \end{bmatrix}.$$

The skew-symmetric matrix  $N_{\mathbf{n}}$  allows us to define the cross-product between a vector  $\mathbf{V}$  and the vector  $\mathbf{n}$ ,

$$\mathbf{V} \times \mathbf{n} = N_{\mathbf{n}}\mathbf{V} \quad \text{and} \quad \mathbf{n} \times \mathbf{V} = N_{\mathbf{n}}^T\mathbf{V}.$$

Moreover, if the vector  $\mathbf{n}$  is normalized, we also have  $N_{\mathbf{n}}^3 = -N_{\mathbf{n}}$ . Using this notation, the matrices  $G_l$ , with  $l$  standing for  $\{x, y, z\}$ , are in fact  $G_l = G_{\mathbf{e}_l}$ , where  $\mathbf{e}_l$ ,  $l = 1, 2, 3$ , are the canonical basis vectors.

We consider here a *total field* formulation, that is, we are interested in the unknown vector  $\mathbf{W} = \mathbf{W}_{\text{inc}} + \mathbf{W}_{\text{sc}}$ , where  $\mathbf{W}_{\text{inc}}$  represents the *incident field* and  $\mathbf{W}_{\text{sc}}$  represents the *scattered field* by an obstacle with boundary  $\Gamma_m$  or in an inhomogeneous medium. Our goal is to solve the boundary-value problem whose strong form is given by

$$\begin{aligned} G_0\mathbf{W} + \sum_{l \in \{x, y, z\}} G_l \partial_l \mathbf{W} &= 0, & \text{in } \Omega, \\ (M_{\Gamma_m} - G_{\mathbf{n}})\mathbf{W} &= 0, & \text{on } \Gamma_m, \\ (M_{\Gamma_a} - G_{\mathbf{n}})(\mathbf{W} - \mathbf{W}_{\text{inc}}) &= 0, & \text{on } \Gamma_a. \end{aligned}$$

Here the matrices  $M_{\Gamma_m}$  and  $M_{\Gamma_a}$  are used for taking into account the boundary conditions of the problem imposed on the *metallic* boundary  $\Gamma_m$  and the *absorbing* boundary  $\Gamma_a$ ,

$$M_{\Gamma_m} = \begin{bmatrix} 0_{3 \times 3} & N_{\mathbf{n}} \\ -N_{\mathbf{n}}^T & 0_{3 \times 3} \end{bmatrix} \quad \text{and} \quad M_{\Gamma_a} = |G_{\mathbf{n}}| = \begin{bmatrix} N_{\mathbf{n}}N_{\mathbf{n}}^T & 0_{3 \times 3} \\ 0_{3 \times 3} & N_{\mathbf{n}}^T N_{\mathbf{n}} \end{bmatrix}.$$

In what follows we will use the matrices  $G_{\mathbf{n}}^+$  and  $G_{\mathbf{n}}^-$ , which denote the positive and negative parts of  $G_{\mathbf{n}}$  according to its diagonalization. We note that  $|G_{\mathbf{n}}| = G_{\mathbf{n}}^+ - G_{\mathbf{n}}^-$ , and the definition of  $G_{\mathbf{n}}^+$  and  $G_{\mathbf{n}}^-$  can be deduced from those of  $G_{\mathbf{n}}$  and  $|G_{\mathbf{n}}|$  by

$$(2.3) \quad G_{\mathbf{n}}^- = \frac{1}{2}(G_{\mathbf{n}} - |G_{\mathbf{n}}|) \quad \text{and} \quad G_{\mathbf{n}}^+ = \frac{1}{2}(G_{\mathbf{n}} + |G_{\mathbf{n}}|).$$

**3. Continuous classical and optimized Schwarz algorithms.** We decompose the computational domain  $\Omega$  into two non-overlapping subdomains  $\Omega_1$  and  $\Omega_2$ . We denote by  $\Sigma$  the interface between  $\Omega_1$  and  $\Omega_2$ , by  $\mathbf{W}_j$  the restriction of  $\mathbf{W}$  to the subdomain  $\Omega_j$ , and by  $\mathbf{n}$  the unit outward normal vector to  $\Sigma$  pointing from  $\Omega_1$  to  $\Omega_2$ . Schwarz algorithms compute at each iteration step  $n = 0, 1, 2, \dots$  a new approximation  $\mathbf{W}_j^{n+1}$  from a given approximation  $\mathbf{W}_j^n$ ,  $j = 1, 2$ , by solving

$$(3.1) \quad \begin{aligned} G_0 \mathbf{W}_1^{n+1} + \sum_{l \in \{x,y,z\}} G_l \partial_l \mathbf{W}_1^{n+1} &= 0, & \text{in } \Omega_1, \\ (G_{\mathbf{n}}^- + S_1 G_{\mathbf{n}}^+) \mathbf{W}_1^{n+1} &= (G_{\mathbf{n}}^- + S_1 G_{\mathbf{n}}^+) \mathbf{W}_2^n, & \text{on } \Sigma, \\ G_0 \mathbf{W}_2^{n+1} + \sum_{l \in \{x,y,z\}} G_l \partial_l \mathbf{W}_2^{n+1} &= 0, & \text{in } \Omega_2, \\ (G_{\mathbf{n}}^+ + S_2 G_{\mathbf{n}}^-) \mathbf{W}_2^{n+1} &= (G_{\mathbf{n}}^+ + S_2 G_{\mathbf{n}}^-) \mathbf{W}_1^n, & \text{on } \Sigma, \end{aligned}$$

where  $S_1$  and  $S_2$  are differential operators. When  $S_1$  and  $S_2$  are equal to zero, the algorithm is called *classical Schwarz algorithm*, and it uses *classical transmission conditions*. It has been shown in [11] that these classical conditions have the meaning of imposing Dirichlet conditions on characteristic (incoming) variables in each subdomain. Since

$$(3.2) \quad G_{\mathbf{n}}^- = \frac{1}{2} \begin{bmatrix} -N_{\mathbf{n}} N_{\mathbf{n}}^T & N_{\mathbf{n}} \\ N_{\mathbf{n}}^T & -N_{\mathbf{n}} N_{\mathbf{n}} \end{bmatrix} = \frac{1}{2} \begin{bmatrix} \mathbb{I}_{3 \times 3} & \\ & -N_{\mathbf{n}}^T \end{bmatrix} \begin{bmatrix} -N_{\mathbf{n}} N_{\mathbf{n}}^T & N_{\mathbf{n}} \end{bmatrix},$$

$$(3.3) \quad G_{\mathbf{n}}^+ = \frac{1}{2} \begin{bmatrix} N_{\mathbf{n}} N_{\mathbf{n}}^T & N_{\mathbf{n}} \\ N_{\mathbf{n}}^T & N_{\mathbf{n}} N_{\mathbf{n}} \end{bmatrix} = \frac{1}{2} \begin{bmatrix} \mathbb{I}_{3 \times 3} & \\ & N_{\mathbf{n}}^T \end{bmatrix} \begin{bmatrix} N_{\mathbf{n}} N_{\mathbf{n}}^T & N_{\mathbf{n}} \end{bmatrix},$$

the classical transmission conditions are also equivalent to imposing impedance conditions,

$$(3.4) \quad \begin{aligned} G_{\mathbf{n}}^- \mathbf{W}_1^{n+1} = G_{\mathbf{n}}^- \mathbf{W}_2^n &\iff \mathcal{B}_{\mathbf{n}}(\mathbf{E}_1^{n+1}, \mathbf{H}_1^{n+1}) = \mathcal{B}_{\mathbf{n}}(\mathbf{E}_2^n, \mathbf{H}_2^n), \\ G_{\mathbf{n}}^+ \mathbf{W}_2^{n+1} = G_{\mathbf{n}}^+ \mathbf{W}_1^n &\iff \mathcal{B}_{-\mathbf{n}}(\mathbf{E}_2^{n+1}, \mathbf{H}_2^{n+1}) = \mathcal{B}_{-\mathbf{n}}(\mathbf{E}_1^n, \mathbf{H}_1^n), \end{aligned}$$

where the impedance operator is given by

$$(3.5) \quad \mathcal{B}_{\mathbf{n}}(\mathbf{E}, \mathbf{H}) := N_{\mathbf{n}} N_{\mathbf{n}}^T \mathbf{E} - N_{\mathbf{n}} \mathbf{H}$$

and for the subdomain  $\Omega_2$  we have used the fact that  $G_{\mathbf{n}}^+ = -G_{-\mathbf{n}}^-$ . The classical Schwarz algorithm has been thoroughly tested in [14] for the solution of the three-dimensional time-harmonic Maxwell's equations discretized by low-order DG methods.

In the second-order formulation of Maxwell's equation, the classical Schwarz method uses the impedance condition

$$(3.6) \quad \tilde{\mathcal{B}}_{\mathbf{n}}(\mathbf{E}) = (\nabla \times \mathbf{E} \times \mathbf{n}) \times \mathbf{n} + i\tilde{\omega} \mathbf{E} \times \mathbf{n};$$

see [9]. This impedance condition is equivalent to using the condition

$$(3.7) \quad \tilde{\mathcal{B}}_{\mathbf{n}}(\mathbf{E}) = (\nabla \times \mathbf{E} \times \mathbf{n}) - i\tilde{\omega} \mathbf{n} \times (\mathbf{E} \times \mathbf{n}),$$

which is just a rotation by 90 degrees of (3.6) but is more adapted to variational formulations; see, for example, [4]. Condition (3.7) is equivalent to (3.5) if we express  $\mathbf{H}$  by Maxwell's equation as a function of  $\nabla \times \mathbf{E}$ . The equivalence between the first- and second-order formulation has been illustrated in [12, 13].

As in (3.4), we also have the equivalences

$$\begin{aligned}
 & (G_{\mathbf{n}}^- + S_1 G_{\mathbf{n}}^+) \mathbf{W}_1^{n+1} = (G_{\mathbf{n}}^- + S_1 G_{\mathbf{n}}^+) \mathbf{W}_2^n \\
 (3.8) \quad & \iff (\mathcal{B}_{\mathbf{n}} + \tilde{S}_1 \mathcal{B}_{-\mathbf{n}}) (\mathbf{E}_1^{n+1}, \mathbf{H}_1^{n+1}) = (\mathcal{B}_{\mathbf{n}} + \tilde{S}_1 \mathcal{B}_{-\mathbf{n}}) (\mathbf{E}_2^n, \mathbf{H}_2^n), \\
 & (G_{\mathbf{n}}^+ + S_2 G_{\mathbf{n}}^-) \mathbf{W}_2^{n+1} = (G_{\mathbf{n}}^+ + S_2 G_{\mathbf{n}}^-) \mathbf{W}_1^n \\
 & \iff (\mathcal{B}_{-\mathbf{n}} + \tilde{S}_2 \mathcal{B}_{\mathbf{n}}) (\mathbf{E}_2^{n+1}, \mathbf{H}_2^{n+1}) = (\mathcal{B}_{-\mathbf{n}} + \tilde{S}_2 \mathcal{B}_{\mathbf{n}}) (\mathbf{E}_1^n, \mathbf{H}_1^n).
 \end{aligned}$$

Here  $\tilde{S}_1$  and  $\tilde{S}_2$  denote differential operators which are approximations of the transparent operators, and  $S_1$  and  $S_2$  are defined to guarantee the above equivalence. In [16], an entire hierarchy of optimized algorithms, defined by the choice of  $\tilde{S}_j$ ,  $j = 1, 2$ , was obtained from the transparent operators. Using (3.2) and (3.3), the optimized transmission conditions (3.8) become

$$\begin{aligned}
 & N_{\mathbf{n}} N_{\mathbf{n}}^T \mathbf{E}_1^{n+1} - N_{\mathbf{n}} \mathbf{H}_1^{n+1} + \tilde{S}_1 (N_{\mathbf{n}} N_{\mathbf{n}}^T \mathbf{E}_1^{n+1} + N_{\mathbf{n}} \mathbf{H}_1^{n+1}) \\
 & \quad = N_{\mathbf{n}} N_{\mathbf{n}}^T \mathbf{E}_2^n - N_{\mathbf{n}} \mathbf{H}_2^n + \tilde{S}_1 (N_{\mathbf{n}} N_{\mathbf{n}}^T \mathbf{E}_2^n + N_{\mathbf{n}} \mathbf{H}_2^n), \\
 & N_{\mathbf{n}} N_{\mathbf{n}}^T \mathbf{E}_2^{n+1} + N_{\mathbf{n}} \mathbf{H}_2^{n+1} + \tilde{S}_2 (N_{\mathbf{n}} N_{\mathbf{n}}^T \mathbf{E}_2^{n+1} - N_{\mathbf{n}} \mathbf{H}_2^{n+1}) \\
 & \quad = N_{\mathbf{n}} N_{\mathbf{n}}^T \mathbf{E}_1^n + N_{\mathbf{n}} \mathbf{H}_1^n + \tilde{S}_2 (N_{\mathbf{n}} N_{\mathbf{n}}^T \mathbf{E}_1^n - N_{\mathbf{n}} \mathbf{H}_1^n).
 \end{aligned}$$

**4. Discontinuous Galerkin approximation.** We now present a weak formulation and a DG discretization of the Schwarz algorithms (3.1) and show how the optimized transmission conditions are properly discretized in a DG framework.

**4.1. Weak formulation.** We denote by  $\mathcal{T}_h$  a triangulation of the domain  $\Omega$ , by  $\Gamma^0$ ,  $\Gamma^m$ , and  $\Gamma^a$ , the sets of purely internal, metallic, and absorbing faces, by  $K$  an element of  $\mathcal{T}_h$ , and by  $F = K \cap \tilde{K}$  the face shared by two neighboring elements  $K$  and  $\tilde{K}$ . On each face  $F$ , we define the *average*  $\{\mathbf{W}\}$  and the *tangential trace jump*  $\llbracket \mathbf{W} \rrbracket$  of  $\mathbf{W}$  by

$$\{\mathbf{W}\} := \frac{1}{2} (\mathbf{W}_K + \mathbf{W}_{\tilde{K}}) \quad \text{and} \quad \llbracket \mathbf{W} \rrbracket := G_{\mathbf{n}_K} \mathbf{W}_K + G_{\mathbf{n}_{\tilde{K}}} \mathbf{W}_{\tilde{K}}.$$

For two vector-valued functions  $\mathbf{U}$  and  $\mathbf{V}$  in  $(L^2(D))^6$ , we introduce the inner products

$$(\mathbf{U}, \mathbf{V})_D := \int_D \mathbf{U} \cdot \bar{\mathbf{V}} \, dx, \quad \langle \mathbf{U}, \mathbf{V} \rangle_F := \int_F \mathbf{U} \cdot \bar{\mathbf{V}} \, ds,$$

for  $D$  being a domain of  $\mathbb{R}^3$  and  $F$  a two-dimensional face. For simplicity, we skip the index for  $\mathcal{T}_h$ , i.e., we write in what follows

$$(\cdot, \cdot) := (\cdot, \cdot)_{\mathcal{T}_h} = \sum_{K \in \mathcal{T}_h} (\cdot, \cdot)_K.$$

On the boundaries we define

$$M_{F,K} := \begin{cases} \begin{bmatrix} \eta_F N_{\mathbf{n}_K} N_{\mathbf{n}_K}^T & N_{\mathbf{n}_K} \\ -N_{\mathbf{n}_K}^T & 0_{3 \times 3} \end{bmatrix} & \text{with } \eta_F \neq 0, \quad \text{if } F \text{ belongs to } \Gamma^m, \\ |G_{\mathbf{n}_K}| & \text{if } F \text{ belongs to } \Gamma^a. \end{cases}$$

We thus obtain a weak formulation of the problem,

$$\begin{aligned}
 & (G_0 \mathbf{W}, \mathbf{V}) + \left( \sum_{l \in \{x,y,z\}} G_l \partial_l \mathbf{W}, \mathbf{V} \right) - \sum_{F \in \Gamma^0} \langle \llbracket \mathbf{W} \rrbracket, \{\mathbf{V}\} \rangle_F + \sum_{F \in \Gamma^0} \langle \frac{1}{2} \llbracket \mathbf{W} \rrbracket, \llbracket \mathbf{V} \rrbracket \rangle_F \\
 & + \sum_{F \in \Gamma^m \cup \Gamma^a} \langle \frac{1}{2} (M_{F,K} - G_{\mathbf{n}_K}) \mathbf{W}, \mathbf{V} \rangle_F = \sum_{F \in \Gamma^a} \langle \frac{1}{2} (M_{F,K} - G_{\mathbf{n}_K}) \mathbf{W}_{\text{inc}}, \mathbf{V} \rangle_F,
 \end{aligned}$$

where we used an upwind flux discretisation [14, equation (4.4)].

**4.2. Discretization of the subdomain problems and the classical Schwarz algorithm.**

Let  $\mathbb{P}_p(D)$  denote the space of polynomial functions of degree at most  $p$  on a domain  $D$ . For any element  $K \in \mathcal{T}_h$ , let  $\mathbf{D}^p(K) \equiv (\mathbb{P}_p(K))^6$ . The discontinuous finite-element spaces we use are then defined by

$$\mathbf{D}_h^p = \left\{ \mathbf{V} \in (L^2(\Omega))^6 \mid \mathbf{V}|_K \in \mathbf{D}^p(K), \forall K \in \mathcal{T}_h \right\}.$$

Approximate solutions  $\mathbf{W}$  and test functions  $\mathbf{V}$  for the discretized problem will be taken in the space  $\mathbf{D}_h^p$ .

Let  $\Gamma_\Sigma$  be the set of faces on the interface  $\Sigma$ ,  $\Gamma_0^j$  be the set of faces in the interior of each subdomain  $\Omega_j$ , and  $\Gamma_b^j$  be the set of faces of each subdomain which lie on the real boundary  $\partial\Omega$ . For any face  $F = K \cap \tilde{K}$ , note also that  $G_{\mathbf{n}_K}^2 = G_{\mathbf{n}_{\tilde{K}}}^2 = |G_{\mathbf{n}_K}| = |G_{\mathbf{n}_{\tilde{K}}}|$ .

Then, for each subdomain  $\Omega_1$  and  $\Omega_2$ , the weak form can be written as

$$(4.1) \quad \begin{aligned} & (G_0 \mathbf{W}_1, \mathbf{V}_1) + \left( \sum_l G_l \partial_l \mathbf{W}_1, \mathbf{V}_1 \right) + \sum_{\Gamma_0^1} \diamond + \sum_{\Gamma_b^1} \diamond \\ & + \sum_{F \in \Gamma_\Sigma} \left\langle \frac{1}{2} (|G_{\mathbf{n}_K}| - G_{\mathbf{n}_K}) (\mathbf{W}_1 - \mathbf{W}_2), \mathbf{V}_1 \right\rangle_F = 0, \\ & (G_0 \mathbf{W}_2, \mathbf{V}_2) + \left( \sum_l G_l \partial_l \mathbf{W}_2, \mathbf{V}_2 \right) + \sum_{\Gamma_0^2} \diamond + \sum_{\Gamma_b^2} \diamond \\ & + \sum_{F \in \Gamma_\Sigma} \left\langle \frac{1}{2} (|G_{\mathbf{n}_{\tilde{K}}}| - G_{\mathbf{n}_{\tilde{K}}}) (\mathbf{W}_2 - \mathbf{W}_1), \mathbf{V}_2 \right\rangle_F = 0, \end{aligned}$$

where, for simplicity, we have replaced some terms on the faces that do not play any particular role in what follows by a  $\diamond$ . For any face  $F = K \cap \tilde{K}$  on  $\Sigma$ , let  $\mathbf{n}$  denote the normal on  $\Sigma$  directed from  $\Omega_1$  towards  $\Omega_2$ , and if  $K$  and  $\tilde{K}$  are elements of  $\Omega_1$  and  $\Omega_2$ , then we have  $\mathbf{n}_K = \mathbf{n} = -\mathbf{n}_{\tilde{K}}$ .

The classical algorithm, which uses characteristic transmission conditions, corresponds in this DG formulation to a simple relaxation of the coupling flux terms in the coupled formulation (4.1): starting from initial guesses  $\mathbf{W}_1^0$  and  $\mathbf{W}_2^0$ , the iterates  $\mathbf{W}_j^{n+1}$  are computed from  $\mathbf{W}_j^n$ ,  $j = 1, 2$ , by solving on  $\Omega_1$  and  $\Omega_2$  the subproblems

$$(4.2) \quad \begin{aligned} & (G_0 \mathbf{W}_1^{n+1}, \mathbf{V}_1) + \left( \sum_l G_l \partial_l \mathbf{W}_1^{n+1}, \mathbf{V}_1 \right) + \sum_{\Gamma_0^1} \diamond + \sum_{\Gamma_b^1} \diamond \\ & + \sum_{F \in \Gamma_\Sigma} \langle G_{\mathbf{n}}^- (\mathbf{W}_1^{n+1} - \mathbf{W}_2^n), \mathbf{V}_1 \rangle_F = 0, \\ & (G_0 \mathbf{W}_2^{n+1}, \mathbf{V}_2) + \left( \sum_l G_l \partial_l \mathbf{W}_2^{n+1}, \mathbf{V}_2 \right) + \sum_{\Gamma_0^2} \diamond + \sum_{\Gamma_b^2} \diamond \\ & + \sum_{F \in \Gamma_\Sigma} \langle G_{\mathbf{n}}^+ (\mathbf{W}_2^{n+1} - \mathbf{W}_1^n), \mathbf{V}_2 \rangle_F = 0, \end{aligned}$$

where we used again (2.3) to simplify the notation. The relaxation in (4.2) is completely natural in the context of a DG discretization: we simply replaced the occurrence of the flux  $G_{\mathbf{n}}^- \mathbf{W}_1^{n+1}$  from outside the subdomain by the flux from the neighboring subdomain  $G_{\mathbf{n}}^- \mathbf{W}_2^n$  at the

previous iteration and vice versa the occurrence of  $G_n^+ \mathbf{W}_2^{n+1}$  by  $G_n^+ \mathbf{W}_1^n$ . This corresponds precisely to using the transmission conditions in (3.1) with  $S_j = 0$ ,  $j = 1, 2$ , namely

$$(4.3) \quad G_n^- \mathbf{W}_1^{n+1} = G_n^- \mathbf{W}_2^n \quad G_n^+ \mathbf{W}_2^{n+1} = G_n^+ \mathbf{W}_1^n,$$

and thus it naturally guarantees that, at convergence of the associated classical Schwarz algorithm, the monodomain DG solution is obtained. Such a simple replacement is, however, not possible for the optimized transmission conditions,  $S_j \neq 0$ . The DG discretization which seems natural for the transmission conditions using the variables available in each subdomain, namely

$$(4.4) \quad \begin{aligned} G_n^- \mathbf{W}_1^{n+1} + S_1 G_n^+ \mathbf{W}_1^{n+1} &= G_n^- \mathbf{W}_2^n + S_1 G_n^+ \mathbf{W}_2^n, \\ G_n^+ \mathbf{W}_2^{n+1} + S_2 G_n^- \mathbf{W}_2^{n+1} &= G_n^+ \mathbf{W}_1^n + S_2 G_n^- \mathbf{W}_1^n, \end{aligned}$$

leads to an obtained solution of the Schwarz algorithm which is different from the monodomain DG solution. The solver should, however, never change the solution sought, and such a discretization is therefore to be avoided. We show in the next section how to properly discretize optimized transmission conditions in the framework of DG discretizations.

**4.3. Discretization of optimized transmission conditions.** In order to correctly introduce optimized transmission conditions (3.1) with a non-zero  $S_j$  into the DG discretization, we first write explicitly what transmission conditions the classical relaxation in (4.2) corresponds to. To do so, the subdomain problems solved in (4.2) are not allowed to depend on variables of the other subdomain anymore since the coupling will be performed with the transmission conditions, and we thus need to introduce additional unknowns, namely  $\mathbf{W}_{2,\Omega_1}^{n+1}$  on  $\Omega_1$  and  $\mathbf{W}_{1,\Omega_2}^{n+1}$  on  $\Omega_2$ , in order to write the classical Schwarz iteration with local variables only, i.e.,

$$(4.5) \quad \begin{aligned} (G_0 \mathbf{W}_1^{n+1}, \mathbf{V}_1) &+ \left( \sum_l G_l \partial_l \mathbf{W}_1^{n+1}, \mathbf{V}_1 \right) + \sum_{\Gamma_0^1} \diamond + \sum_{\Gamma_b^1} \diamond \\ &- \sum_{F \in \Gamma_\Sigma} \left\langle G_n^- (\mathbf{W}_1^{n+1} - \mathbf{W}_{2,\Omega_1}^{n+1}), \mathbf{V}_1 \right\rangle_F = 0, \\ (G_0 \mathbf{W}_2^{n+1}, \mathbf{V}_2) &+ \left( \sum_l G_l \partial_l \mathbf{W}_2^{n+1}, \mathbf{V}_2 \right) + \sum_{\Gamma_0^2} \diamond + \sum_{\Gamma_b^2} \diamond \\ &+ \sum_{F \in \Gamma_\Sigma} \left\langle G_n^+ (\mathbf{W}_2^{n+1} - \mathbf{W}_{1,\Omega_2}^{n+1}), \mathbf{V}_2 \right\rangle_F = 0. \end{aligned}$$

Comparing with the classical Schwarz algorithm (4.2), we see that in order to obtain the same algorithm, the transmission conditions for (4.5) need to be chosen as

$$(4.6) \quad G_n^- \mathbf{W}_{2,\Omega_1}^{n+1} = G_n^- \mathbf{W}_2^n, \quad G_n^+ \mathbf{W}_{1,\Omega_2}^{n+1} = G_n^+ \mathbf{W}_1^n,$$

which we have already encountered when explicitly stating the relaxation as a replacement in (4.3). But one has to be careful when keeping these variables since they represent the outside traces at the interface, not the inside traces of the elements! The transmission condition (4.6) implies that in the limit, when the algorithm converges, the so-called *coupling conditions*

$$(4.7) \quad G_n^- \mathbf{W}_{2,\Omega_1} = G_n^- \mathbf{W}_2, \quad G_n^+ \mathbf{W}_{1,\Omega_2} = G_n^+ \mathbf{W}_1,$$

will be satisfied, where we dropped the iteration index to denote the limit quantities. These are the conditions which imply the equivalence of the converged solution to the monodomain

DG solution. When using the Schwarz algorithm (4.5) with the optimized transmission conditions (3.1), we therefore propose to use DG discretizations of the strong relations

$$(4.8) \quad \begin{aligned} G_{\mathbf{n}}^- \mathbf{W}_{2,\Omega_1}^{n+1} + S_1 G_{\mathbf{n}}^+ \mathbf{W}_1^{n+1} &= G_{\mathbf{n}}^- \mathbf{W}_2^n + S_1 G_{\mathbf{n}}^+ \mathbf{W}_{1,\Omega_2}^n, \\ G_{\mathbf{n}}^+ \mathbf{W}_{1,\Omega_2}^{n+1} + S_2 G_{\mathbf{n}}^- \mathbf{W}_2^{n+1} &= G_{\mathbf{n}}^+ \mathbf{W}_1^n + S_2 G_{\mathbf{n}}^- \mathbf{W}_{2,\Omega_1}^n, \end{aligned}$$

which are substantially different from the transmission conditions (4.4) since they use additional variables  $\mathbf{W}_{2,\Omega_1}$  and  $\mathbf{W}_{1,\Omega_2}$ , which in principle belong to the traces at the interface  $\Sigma$  of the neighboring subdomain and are not available in the formulation (4.4). We now prove that with the transmission conditions (4.8), at convergence of the associated Schwarz algorithm, the same coupling conditions as (4.7) hold, and thus the optimized Schwarz method converges to the monodomain solution of the chosen DG discretization. First, from (3.2) and (3.3), note that relation (4.7) is equivalent to

$$\begin{aligned} N_{\mathbf{n}} N_{\mathbf{n}}^T \mathbf{E}_{2,\Omega_1} - N_{\mathbf{n}} \mathbf{H}_{2,\Omega_1} &= N_{\mathbf{n}} N_{\mathbf{n}}^T \mathbf{E}_2 - N_{\mathbf{n}} \mathbf{H}_2, \\ N_{\mathbf{n}} N_{\mathbf{n}}^T \mathbf{E}_{1,\Omega_2} + N_{\mathbf{n}} \mathbf{H}_{1,\Omega_2} &= N_{\mathbf{n}} N_{\mathbf{n}}^T \mathbf{E}_1 + N_{\mathbf{n}} \mathbf{H}_1. \end{aligned}$$

We now introduce the auxiliary variables

$$\begin{aligned} \Lambda_{2,\Omega_1} &:= N_{\mathbf{n}} N_{\mathbf{n}}^T \mathbf{E}_{2,\Omega_1} - N_{\mathbf{n}} \mathbf{H}_{2,\Omega_1}, & \Lambda_2 &:= N_{\mathbf{n}} N_{\mathbf{n}}^T \mathbf{E}_2 - N_{\mathbf{n}} \mathbf{H}_2, \\ \Lambda_{1,\Omega_2} &:= N_{\mathbf{n}} N_{\mathbf{n}}^T \mathbf{E}_{1,\Omega_2} + N_{\mathbf{n}} \mathbf{H}_{1,\Omega_2}, & \Lambda_1 &:= N_{\mathbf{n}} N_{\mathbf{n}}^T \mathbf{E}_1 + N_{\mathbf{n}} \mathbf{H}_1. \end{aligned}$$

These variables represent traces belonging to a trace finite-element space

$$M_h^p = \left\{ \boldsymbol{\eta} \in (L^2(\Sigma))^3 \mid \boldsymbol{\eta}|_F \in (\mathbb{P}_p(F))^3, (\boldsymbol{\eta} \cdot \mathbf{n})|_F = 0, \forall F \in \Sigma \right\}.$$

Note that  $M_h^p$  consists of vector-valued functions whose normal component is zero on any face  $F \in \Sigma$ . At convergence of the classical Schwarz algorithm and hence for the monodomain DG solution, we see from (4.7) that these trace variables have to satisfy

$$(4.9) \quad \Lambda_{2,\Omega_1} = \Lambda_2, \quad \Lambda_{1,\Omega_2} = \Lambda_1.$$

From (4.8) and (4.9), we have to find for the optimized transmission conditions a suitable DG discretization of the relations

$$(4.10) \quad \Lambda_{2,\Omega_1} + \tilde{S}_1 \Lambda_1 = \Lambda_2 + \tilde{S}_1 \Lambda_{1,\Omega_2}, \quad \Lambda_{1,\Omega_2} + \tilde{S}_2 \Lambda_2 = \Lambda_1 + \tilde{S}_2 \Lambda_{2,\Omega_1}.$$

We therefore need to give now the precise expressions used in optimized Schwarz methods for the operators  $\tilde{S}_j$ ,  $j = 1, 2$ . Several choices for these operators have been proposed in [16] based on Fourier analysis under the assumption that the interface is a plane: they are second-order differential operators in the tangential direction of the interface, whose Fourier symbols are given in Table 4.1, where  $\mathcal{F}$  denotes the Fourier transform and  $\mathbf{k}$  is the Fourier parameter in the tangential direction of the interface. The matrix-valued operators  $\tilde{Q}_{s_j}$  are given by

$$\tilde{Q}_{s_j} = \begin{bmatrix} \partial_{\tau_1 \tau_1} - \partial_{\tau_2 \tau_2} - \tilde{\sigma} s_j & 2\partial_{\tau_1 \tau_2} \\ 2\partial_{\tau_1 \tau_2} & \partial_{\tau_2 \tau_2} - \partial_{\tau_1 \tau_1} - \tilde{\sigma} s_j \end{bmatrix},$$

and the division by  $|\mathbf{k}|^2$  indicates an integral operation. We explain below how this integration can be avoided in the implementation. Every choice in Table 4.1 leads to a different transmission condition and thus a different optimized Schwarz algorithm. Note that the operator  $\tilde{Q}_{s_j}$



TABLE 4.1  
*Symbols of the different operators for 3D Maxwell's equations.*

Algorithm	$\mathcal{F}(\tilde{S}_j)$
1	0
2	$\frac{s-i\tilde{\omega}}{(s+i\tilde{\omega})( \mathbf{k} ^2+s\tilde{\sigma})} \mathcal{F}(\tilde{Q}_s), \quad s \in \mathbb{C}$
3	$\frac{1}{ \mathbf{k} ^2-2\tilde{\omega}^2+2i\tilde{\omega}\tilde{\sigma}+(2i\tilde{\omega}+\tilde{\sigma})s} \mathcal{F}(\tilde{Q}_s), \quad s \in \mathbb{C}$
4	$\frac{s_j-i\tilde{\omega}}{(s_j+i\tilde{\omega})( \mathbf{k} ^2+s_j\tilde{\sigma})} \mathcal{F}(\tilde{Q}_{s_j}), \quad s_j \in \mathbb{C}$
5	$\frac{1}{ \mathbf{k} ^2-2\tilde{\omega}^2+2i\tilde{\omega}\tilde{\sigma}+(2i\tilde{\omega}+\tilde{\sigma})s_j} \mathcal{F}(\tilde{Q}_{s_j}), \quad s_j \in \mathbb{C}$

can be rewritten in a more natural form for Maxwell's equations,

$$\begin{aligned} \tilde{Q}_{s_j} &= \begin{bmatrix} \partial_{\tau_1\tau_1} & \partial_{\tau_1\tau_2} \\ \partial_{\tau_1\tau_2} & \partial_{\tau_2\tau_2} \end{bmatrix} + \begin{bmatrix} -\partial_{\tau_2\tau_2} & \partial_{\tau_1\tau_2} \\ \partial_{\tau_1\tau_2} & -\partial_{\tau_1\tau_1} \end{bmatrix} - \tilde{\sigma}s_j \mathbf{I} \\ &= \underbrace{\nabla_\tau \nabla_\tau \cdot}_{\mathcal{S}_{TM}} + \underbrace{\nabla_\tau \times \nabla_\tau \times}_{\mathcal{S}_{TE}} - \tilde{\sigma}s_j \mathbf{I}, \end{aligned}$$

where  $\mathbf{I}$  denotes the identity operator,  $\tau_j$ ,  $j = 1, 2$ , are two independent vectors in the tangent plane to the interface,  $\nabla_\tau$  denotes the gradient in the tangent plane to the interface,  $\nabla_\tau \cdot$  is the divergence in the tangent plane, and  $\nabla_\tau \times$  is the two-dimensional curl operator in the tangent plane. The operators  $\mathcal{S}_{TM}$  and  $\mathcal{S}_{TE}$  satisfy the remarkable relation

$$-\Delta_\tau \mathbf{I} = \mathcal{S}_{TE} - \mathcal{S}_{TM},$$

where  $\Delta_\tau$  is the Laplace-Beltrami operator, and they act mainly on the transverse electric and transverse magnetic part of the solution; see [12, 13] for a more detailed explanation.

To avoid an integral relation in the transmission condition, one has to multiply the entire transmission conditions by the operator symbol in the denominator and then obtains second-order differential transmission conditions. These second-order differential transmission conditions are equivalent to the transmission conditions (4.10) and are of the form

$$(4.11) \quad \begin{aligned} \tilde{P}_1(\Lambda_{2,\Omega_1} - \Lambda_2) &= \tilde{Q}_{s_1}(\Lambda_{1,\Omega_2} - \Lambda_1), \\ \tilde{P}_2(\Lambda_{1,\Omega_2} - \Lambda_1) &= \tilde{Q}_{s_2}(\Lambda_{2,\Omega_1} - \Lambda_2), \end{aligned}$$

where, for example for Algorithms 2 and 4 indicated in Table 4.1, we have

$$(4.12) \quad \tilde{P}_j := \frac{s_j + i\tilde{\omega}}{s_j - i\tilde{\omega}} (-\Delta_\tau + \tilde{\sigma}s_j) \mathbf{I}, \quad s_j \in \mathbb{C},$$

and for Algorithms 3 and 5 in Table 4.1, we have

$$(4.13) \quad \begin{aligned} \tilde{P}_j &:= (-\Delta_\tau - 2\tilde{\omega}^2 + 2i\tilde{\omega}\tilde{\sigma} + 2i\tilde{\omega}s_j + \tilde{\sigma}s_j) \mathbf{I} \\ &= \mathcal{S}_{TE} - \mathcal{S}_{TM} + (-2\tilde{\omega}^2 + 2i\tilde{\omega}\tilde{\sigma} + 2i\tilde{\omega}s_j + \tilde{\sigma}s_j) \mathbf{I}, \quad s_j \in \mathbb{C}. \end{aligned}$$

We see that even though these transmission conditions have been derived in [16] assuming that the interface is planar, their reformulation allows us to use them also for non-planar interfaces obtained for example by an automatic mesh partitioning tool in the context of DG discretizations.

TABLE 4.2

*Asymptotic convergence factor and optimized choice of the parameters in the transmission conditions for the 3D Maxwell's equations.*

Algorithm	with overlap, $L = h$	
	$\rho$	parameters
1	$1 - \frac{4}{3} (9\tilde{\omega}^4 \tilde{\sigma}^2)^{\frac{1}{8}} h^{\frac{3}{4}}$	none
2	$1 - 2^{\frac{7}{6}} (\tilde{\omega} \tilde{\sigma})^{1/6} h^{\frac{1}{3}}$	$p = \frac{(2\tilde{\omega} \tilde{\sigma})^{1/3}}{2h^{\frac{1}{3}}}$
3	$1 - \frac{2^{\frac{17}{10}} (\tilde{\omega}^4 \tilde{\sigma}^2)^{\frac{1}{20}} h^{\frac{3}{10}}}{3^{\frac{3}{10}}}$	$p = \frac{2^{\frac{2}{5}} (\tilde{\omega}^4 \tilde{\sigma}^2)^{\frac{1}{10}}}{3^{\frac{3}{5}} h^{\frac{2}{5}}}$
4	$1 - 4\sqrt{2} (\tilde{\omega} \tilde{\sigma})^{\frac{1}{10}} h^{\frac{1}{5}}$	$p_1 = \frac{(\tilde{\omega} \tilde{\sigma})^{\frac{1}{5}}}{2h^{\frac{3}{5}}}, p_2 = \frac{(\tilde{\omega} \tilde{\sigma})^{\frac{2}{5}}}{2h^{\frac{1}{5}}}$
5	$1 - \frac{2^{\frac{23}{8}} (\tilde{\omega}^4 \tilde{\sigma}^2)^{\frac{1}{32}} h^{\frac{3}{16}}}{3^{\frac{3}{16}}}$	$p_1 = \frac{(\tilde{\omega}^4 \tilde{\sigma}^2)^{\frac{1}{16}}}{2^{\frac{1}{4}} 3^{\frac{3}{8}} h^{\frac{5}{8}}}, p_2 = \frac{\sqrt{2}(\tilde{\omega}^4 \tilde{\sigma}^2)^{\frac{1}{8}}}{3^{\frac{3}{4}} h^{\frac{1}{4}}}$
without overlap, $L = 0$		
1	$1 - \frac{\tilde{\omega}^2 \tilde{\sigma} h^3}{C^3}$	none
2	$1 - \frac{2^{\frac{3}{4}} (\tilde{\omega} \tilde{\sigma})^{\frac{1}{4}} \sqrt{h}}{\sqrt{C}}$	$p = \frac{(\tilde{\omega} \tilde{\sigma})^{\frac{1}{4}} \sqrt{C}}{2^{\frac{1}{4}} \sqrt{h}}$
3	$1 - \frac{2^{\frac{11}{7}} (\tilde{\omega}^4 \tilde{\sigma}^2)^{\frac{1}{14}} h^{\frac{3}{7}}}{3^{\frac{3}{7}} C^{\frac{3}{7}}}$	$p = \frac{2^{\frac{4}{7}} (\tilde{\omega}^4 \tilde{\sigma}^2)^{\frac{1}{14}} C^{\frac{4}{7}}}{3^{\frac{3}{7}} h^{\frac{4}{7}}}$
4	$1 - \frac{(2\tilde{\omega} \tilde{\sigma})^{\frac{1}{8}} h^{\frac{1}{4}}}{C^{\frac{1}{4}}}$	$p_1 = \frac{(2\tilde{\omega} \tilde{\sigma})^{\frac{1}{8}} C^{\frac{3}{4}}}{h^{\frac{3}{4}}}, p_2 = \frac{(2\tilde{\omega} \tilde{\sigma})^{3/8} C^{1/4}}{2h^{\frac{1}{4}}}$
5	$1 - \frac{2^{\frac{34}{13}} (\tilde{\omega}^4 \tilde{\sigma}^2)^{\frac{1}{26}} h^{\frac{3}{13}}}{3^{\frac{3}{13}} C^{\frac{3}{13}}}$	$p_1 = \frac{2^{\frac{8}{13}} (\tilde{\omega}^4 \tilde{\sigma}^2)^{\frac{1}{26}} C^{\frac{10}{13}}}{3^{\frac{3}{13}} h^{\frac{10}{13}}}, p_2 = \frac{2^{\frac{11}{13}} (\tilde{\omega}^4 \tilde{\sigma}^2)^{\frac{3}{26}} C^{\frac{4}{13}}}{3^{\frac{9}{13}} h^{\frac{4}{13}}}$

It remains to choose the parameters  $s_j, j = 1, 2$ , in (4.12) and (4.13) to complete the definition of the corresponding optimized Schwarz method. These parameters are selected by a minimization of the associated contraction factors for a model problem such that the performance of the method is optimized, and we show for completeness in Table 4.2 the optimized values from [16] adapted to the notation in this manuscript.

Having defined all the components in the transmission conditions (4.11), we now explain how to discretize the five variants in a consistent fashion using a DG discretization: let  $(\boldsymbol{\eta}_j)_j$  be a basis of  $M_h^p$ . On the interface  $\Sigma$  we define the matrices

$$(M_\Sigma)_{i,j} := \sum_{F \in \Sigma} \langle \boldsymbol{\eta}_i, \boldsymbol{\eta}_j \rangle_F,$$

$$\begin{aligned}
 (K_\Sigma)_{i,j} := & \sum_{F \in \Sigma} \langle \nabla_\tau \times \boldsymbol{\eta}_i, \nabla_\tau \times \boldsymbol{\eta}_j \rangle_F + \langle \nabla_\tau \cdot \boldsymbol{\eta}_i, \nabla_\tau \cdot \boldsymbol{\eta}_j \rangle_F \\
 & + \sum_{e \in \partial \Sigma} \int_e \alpha h^{-1} \sum_{k \in \{1,2\}} [[[\boldsymbol{\eta}_i \cdot \boldsymbol{\tau}_k]]][[\boldsymbol{\eta}_j \cdot \boldsymbol{\tau}_k]] \\
 & - \sum_{e \in \partial \Sigma} \int_e \{ \{ \nabla_\tau \cdot \boldsymbol{\eta}_i \} \} [[[\boldsymbol{\eta}_j \cdot \boldsymbol{n}_{e,\tau}]]] - [[[\boldsymbol{\eta}_i \cdot \boldsymbol{n}_{e,\tau}]]] \{ \{ \nabla_\tau \cdot \boldsymbol{\eta}_j \} \} \\
 & - \sum_{e \in \partial \Sigma} \int_e \{ \{ \nabla_\tau \times \boldsymbol{\eta}_i \} \} \cdot [[[\boldsymbol{\eta}_j \times \boldsymbol{n}_{e,\tau}]]] - [[[\boldsymbol{\eta}_i \times \boldsymbol{n}_{e,\tau}]]] \cdot \{ \{ \nabla_\tau \times \boldsymbol{\eta}_j \} \},
 \end{aligned}$$

and

$$\begin{aligned}
 (A_\Sigma)_{i,j} := & \sum_{F \in \Sigma} \langle \nabla_\tau \times \boldsymbol{\eta}_i, \nabla_\tau \times \boldsymbol{\eta}_j \rangle_F - \langle \nabla_\tau \cdot \boldsymbol{\eta}_i, \nabla_\tau \cdot \boldsymbol{\eta}_j \rangle_F \\
 & + \sum_{e \in \partial \Sigma} \int_e \alpha h^{-1} \sum_{k \in \{1,2\}} \llbracket \boldsymbol{\eta}_i \cdot \boldsymbol{\tau}_k \rrbracket \llbracket \boldsymbol{\eta}_j \cdot \boldsymbol{\tau}_k \rrbracket \\
 & + \sum_{e \in \partial \Sigma} \int_e \{ \{ \nabla_\tau \cdot \boldsymbol{\eta}_i \} \} \llbracket \boldsymbol{\eta}_j \cdot \boldsymbol{n}_{e,\tau} \rrbracket - \llbracket \boldsymbol{\eta}_i \cdot \boldsymbol{n}_{e,\tau} \rrbracket \{ \{ \nabla_\tau \cdot \boldsymbol{\eta}_j \} \}, \\
 & - \sum_{e \in \partial \Sigma} \int_e \{ \{ \nabla_\tau \times \boldsymbol{\eta}_i \} \} \cdot \llbracket \boldsymbol{\eta}_j \times \boldsymbol{n}_{e,\tau} \rrbracket - \llbracket \boldsymbol{\eta}_i \times \boldsymbol{n}_{e,\tau} \rrbracket \cdot \{ \{ \nabla_\tau \times \boldsymbol{\eta}_j \} \},
 \end{aligned}$$

where the positivity of the discretized operator is guaranteed for sufficiently large  $\alpha$ ,  $\partial \Sigma$  denotes the set of interior edges of  $\Sigma$ ,  $\llbracket \cdot \rrbracket$  and  $\{ \{ \cdot \} \}$  denote the jump and the average at an edge  $e$  of the values at neighboring triangles, and  $\boldsymbol{n}_{e,\tau}$  is the outward normal on  $e$  in the tangent plane. Then matrix  $K_\Sigma$  stems from the discretization of  $-\Delta_\tau$  using a symmetric interior penalty approach [2, 3]. Note that the operator  $-\Delta_\tau$  has to be taken in “vector” form since it is applied to  $(\Lambda_{2,\Omega_1} - \Lambda_2)$ , which is a discretization of a vector quantity.  $M_\Sigma$  is an interface mass matrix with the same dimensions as the interface stiffness matrix  $K_\Sigma$ , and  $A_\Sigma$  represents the discretization of the operator

$$\begin{bmatrix} \partial_{\tau_1 \tau_1} - \partial_{\tau_2 \tau_2} & 2\partial_{\tau_1 \tau_2} \\ 2\partial_{\tau_1 \tau_2} & \partial_{\tau_2 \tau_2} - \partial_{\tau_1 \tau_1} \end{bmatrix}.$$

Then the DG discretization of (4.11) for the Algorithms 2 and 4 is

$$\begin{aligned}
 \frac{s_1 + i\tilde{\omega}}{s_1 - i\tilde{\omega}} (K_\Sigma + \tilde{\sigma} s_1 M_\Sigma) (\Lambda_{2,\Omega_1} - \Lambda_2) &= (A_\Sigma - \tilde{\sigma} s_1 M_\Sigma) (\Lambda_{1,\Omega_2} - \Lambda_1), \\
 \frac{s_2 + i\tilde{\omega}}{s_2 - i\tilde{\omega}} (K_\Sigma + \tilde{\sigma} s_2 M_\Sigma) (\Lambda_{1,\Omega_2} - \Lambda_1) &= (A_\Sigma - \tilde{\sigma} s_2 M_\Sigma) (\Lambda_{2,\Omega_1} - \Lambda_2),
 \end{aligned}$$

and for the Algorithms 3 and 5 we get

$$\begin{aligned}
 (4.14) \quad & (K_\Sigma + \alpha_1 M_\Sigma) (\Lambda_{2,\Omega_1} - \Lambda_2) = (A_\Sigma - \tilde{\sigma} s_1 M_\Sigma) (\Lambda_{1,\Omega_2} - \Lambda_1), \\
 & (K_\Sigma + \alpha_2 M_\Sigma) (\Lambda_{1,\Omega_2} - \Lambda_1) = (A_\Sigma - \tilde{\sigma} s_2 M_\Sigma) (\Lambda_{2,\Omega_1} - \Lambda_2),
 \end{aligned}$$

where  $\alpha_j = 2i\tilde{\omega}(i\tilde{\omega} + \tilde{\sigma}) + 2i\tilde{\omega}s_j + \tilde{\sigma}s_j$ . In the following theorem we will only treat the case of Algorithms 3 and 5; similar techniques can be applied for Algorithms 2 and 4.

**THEOREM 4.1** (DG discretization of Algorithms 3 and 5). *If  $s_1$  and  $s_2$  are such that  $s_j = p_j(1 + i)$  with  $p_j$  a strictly positive real number for  $j = 1, 2$ , and  $\tilde{\sigma}(p_1 - p_2) = 0$ , then the relations (4.9) and (4.14) are equivalent.*

*Proof.* We first observe that  $\Im \alpha_j = 2\tilde{\omega}\tilde{\sigma} + 2\tilde{\omega}p_j + \tilde{\sigma}p_j > 0$ . Let us denote

$$\mathbf{U}_1 = \Lambda_{1,\Omega_2} - \Lambda_1, \quad \mathbf{U}_2 = \Lambda_{2,\Omega_1} - \Lambda_2.$$

Multiplying the first relation in (4.14) on the left by  $\bar{\mathbf{U}}_2^T$  and the second by  $\bar{\mathbf{U}}_1^T$  and summing them up, we get

$$\begin{aligned}
 & \bar{\mathbf{U}}_2^T (K_\Sigma + \alpha_1 M_\Sigma) \mathbf{U}_2 + \bar{\mathbf{U}}_1^T (K_\Sigma + \alpha_2 M_\Sigma) \mathbf{U}_1 \\
 & = \bar{\mathbf{U}}_2^T (A_\Sigma - \tilde{\sigma} s_1 M_\Sigma) \mathbf{U}_1 + \bar{\mathbf{U}}_1^T (A_\Sigma - \tilde{\sigma} s_2 M_\Sigma) \mathbf{U}_2.
 \end{aligned}$$

Since  $K_\Sigma$  is symmetric and non-negative,  $M_\Sigma$  is symmetric and positive definite, and  $A_\Sigma$  is symmetric, all the quantities  $\bar{\mathbf{U}}_j^T M_\Sigma \mathbf{U}_j$ ,  $\bar{\mathbf{U}}_j^T K_\Sigma \mathbf{U}_j$ , and  $\bar{\mathbf{U}}_1^T A_\Sigma \mathbf{U}_2 + \bar{\mathbf{U}}_2^T A_\Sigma \mathbf{U}_1$  are real. In this case, by taking the imaginary part of the previous relation, we get

$$(4.15) \quad \Im \alpha_1 \bar{\mathbf{U}}_2^T M_\Sigma \mathbf{U}_2 + \Im \alpha_2 \bar{\mathbf{U}}_1^T M_\Sigma \mathbf{U}_1 + \tilde{\sigma} \Im (s_1 \bar{\mathbf{U}}_2^T M_\Sigma \mathbf{U}_1 + s_2 \bar{\mathbf{U}}_1^T M_\Sigma \mathbf{U}_2) = 0.$$

In order to simplify notation and by using that  $M_\Sigma$  is symmetric positive definite, we introduce the norm  $\|\mathbf{U}\|_{M_\Sigma}^2 := \bar{\mathbf{U}}^T M_\Sigma \mathbf{U}$  induced by the Hermitian product  $(\mathbf{U}_1, \mathbf{U}_2)_{M_\Sigma} = \bar{\mathbf{U}}_2^T M_\Sigma \mathbf{U}_1$ . Since by definition  $(\mathbf{U}_2, \mathbf{U}_1)_{M_\Sigma} = \overline{(\mathbf{U}_1, \mathbf{U}_2)_{M_\Sigma}}$ , we see that

$$\begin{aligned} \Im(\bar{\mathbf{U}}_2^T M_\Sigma \mathbf{U}_1) &= \frac{1}{2i}((\mathbf{U}_1, \mathbf{U}_2)_{M_\Sigma} - (\mathbf{U}_2, \mathbf{U}_1)_{M_\Sigma}) = -\Im(\bar{\mathbf{U}}_1^T M_\Sigma \mathbf{U}_2), \\ \Re(\bar{\mathbf{U}}_2^T M_\Sigma \mathbf{U}_1) &= \frac{1}{2}((\mathbf{U}_1, \mathbf{U}_2)_{M_\Sigma} + (\mathbf{U}_2, \mathbf{U}_1)_{M_\Sigma}) = \Re(\bar{\mathbf{U}}_1^T M_\Sigma \mathbf{U}_2), \\ \Im(s_1 \bar{\mathbf{U}}_2^T M_\Sigma \mathbf{U}_1) &= p_1(\Re(\mathbf{U}_1, \mathbf{U}_2)_{M_\Sigma} + \Im(\mathbf{U}_1, \mathbf{U}_2)_{M_\Sigma}), \\ \Im(s_2 \bar{\mathbf{U}}_1^T M_\Sigma \mathbf{U}_2) &= p_2(\Re(\mathbf{U}_2, \mathbf{U}_1)_{M_\Sigma} + \Im(\mathbf{U}_2, \mathbf{U}_1)_{M_\Sigma}) \\ &= p_2(\Re(\mathbf{U}_1, \mathbf{U}_2)_{M_\Sigma} - \Im(\mathbf{U}_1, \mathbf{U}_2)_{M_\Sigma}). \end{aligned}$$

Also, let  $p_1 = p + \delta$  and  $p_2 = p - \delta$ , and suppose that  $\delta \geq 0$ . Then (4.15) becomes

$$\begin{aligned} &2\tilde{\omega}(\tilde{\sigma} + p_1)\|\mathbf{U}_2\|_{M_\Sigma}^2 + 2\tilde{\omega}(\tilde{\sigma} + p_2)\|\mathbf{U}_1\|_{M_\Sigma}^2 + \tilde{\sigma}(p + \delta)\|\mathbf{U}_2\|_{M_\Sigma}^2 \\ &\quad + \tilde{\sigma}(p - \delta)\|\mathbf{U}_1\|_{M_\Sigma}^2 + \tilde{\sigma}(p + \delta)(\Re(\mathbf{U}_1, \mathbf{U}_2)_{M_\Sigma} + \Im(\mathbf{U}_1, \mathbf{U}_2)_{M_\Sigma}) \\ &\quad + \tilde{\sigma}(p - \delta)(\Re(\mathbf{U}_1, \mathbf{U}_2)_{M_\Sigma} - \Im(\mathbf{U}_1, \mathbf{U}_2)_{M_\Sigma}) = 0 \\ (4.16) \quad \Leftrightarrow &2\tilde{\omega}(\tilde{\sigma} + p_1)\|\mathbf{U}_2\|_{M_\Sigma}^2 + 2\tilde{\omega}(\tilde{\sigma} + p_2)\|\mathbf{U}_1\|_{M_\Sigma}^2 \\ &\quad + \tilde{\sigma}p(\|\mathbf{U}_2\|_{M_\Sigma}^2 + \|\mathbf{U}_1\|_{M_\Sigma}^2 + 2\Re(\mathbf{U}_1, \mathbf{U}_2)_{M_\Sigma}) \\ &\quad + \tilde{\sigma}\delta(\|\mathbf{U}_2\|_{M_\Sigma}^2 - \|\mathbf{U}_1\|_{M_\Sigma}^2 + 2\Im(\mathbf{U}_1, \mathbf{U}_2)_{M_\Sigma}) = 0 \\ \Leftrightarrow &2\tilde{\omega}(\tilde{\sigma} + p_1)\|\mathbf{U}_2\|_{M_\Sigma}^2 + 2\tilde{\omega}(\tilde{\sigma} + p_2)\|\mathbf{U}_1\|_{M_\Sigma}^2 + \tilde{\sigma}p\|\mathbf{U}_1 + \mathbf{U}_2\|_{M_\Sigma}^2 \\ &\quad + \tilde{\sigma}\delta(\|\mathbf{U}_2\|_{M_\Sigma}^2 - \|\mathbf{U}_1\|_{M_\Sigma}^2 + 2\Im(\mathbf{U}_1, \mathbf{U}_2)_{M_\Sigma}) = 0. \end{aligned}$$

We thus see that if  $\tilde{\sigma} = 0$  or  $\delta = 0$ , which means that  $p_1 = p_2$  (Algorithm 3 from Table 4.2), then the last form of (4.16) leads to the conclusion that  $\mathbf{U}_j = 0$  since all the terms are positive, which proves the equivalence between (4.14) and (4.9).  $\square$

**4.4. The two-dimensional case.** As in the three-dimensional case, we can rewrite (4.8) and (4.7) by introducing the auxiliary variables (see [17] for more details)

$$(4.17) \quad \begin{aligned} \Lambda_{2,\Omega_1} &:= E_{2,\Omega_1} - N_{\mathbf{n}}\mathbf{H}_{2,\Omega_1}, & \Lambda_2 &:= E_2 - N_{\mathbf{n}}\mathbf{H}_2, \\ \Lambda_{1,\Omega_2} &:= E_{1,\Omega_2} + N_{\mathbf{n}}\mathbf{H}_{1,\Omega_2}, & \Lambda_1 &:= E_1 + N_{\mathbf{n}}\mathbf{H}_1, \end{aligned}$$

belonging to the trace space  $M_h^p = \{\eta \in L^2(\Sigma) \mid \eta|_F \in \mathbb{P}_p(F), \forall F \in \Sigma\}$ . Then (4.7) becomes

$$(4.18) \quad \Lambda_{2,\Omega_1} = \Lambda_2 \quad \text{and} \quad \Lambda_{1,\Omega_2} = \Lambda_1.$$

From (4.8) and (4.17), we see that for the optimized transmission conditions, we have to find a suitable DG discretization of the relations

$$(4.19) \quad \Lambda_{2,\Omega_1} + \tilde{S}_1 \Lambda_1 = \Lambda_2 + \tilde{S}_1 \Lambda_{1,\Omega_2} \quad \text{and} \quad \Lambda_{1,\Omega_2} + \tilde{S}_2 \Lambda_2 = \Lambda_1 + \tilde{S}_2 \Lambda_{2,\Omega_1}.$$

If we focus on the second-order transmission conditions, (4.19) becomes

$$(4.20) \quad \begin{aligned} &(-\partial_\tau^2 + i\tilde{\omega}\tilde{\sigma} - 2\tilde{\omega}^2 + 2i\tilde{\omega}s_1)(\Lambda_{2,\Omega_1} - \Lambda_2) + (-\partial_\tau^2 + i\tilde{\omega}\tilde{\sigma})(\Lambda_{1,\Omega_2} - \Lambda_1) = 0, \\ &(-\partial_\tau^2 + i\tilde{\omega}\tilde{\sigma} - 2\tilde{\omega}^2 + 2i\tilde{\omega}s_2)(\Lambda_{1,\Omega_2} - \Lambda_1) + (-\partial_\tau^2 + i\tilde{\omega}\tilde{\sigma})(\Lambda_{2,\Omega_1} - \Lambda_2) = 0. \end{aligned}$$

Let  $(\eta_j)_j$  be a basis of  $M_h^p$ . We define the matrices

$$\begin{aligned} (M_\Sigma)_{i,j} &:= \sum_{F \in \Sigma} \langle \eta_i, \eta_j \rangle_F, \\ (K_\Sigma)_{i,j} &:= \sum_{F \in \Sigma} \langle \partial_\tau \eta_i, \partial_\tau \eta_j \rangle_F + \sum_{n \in \Sigma^0} \alpha_n h^{-1} \{ \{ \{ \{ \eta_i \} \} \} \}_n \{ \{ \{ \{ \eta_j \} \} \} \}_n \\ &\quad - \sum_{n \in \Sigma^0} \{ \{ \partial_\tau \eta_i \} \}_n \{ \{ \{ \{ \eta_j \} \} \} \}_n - \{ \{ \{ \{ \eta_i \} \} \} \}_n \{ \{ \partial_\tau \eta_j \} \}_n, \end{aligned}$$

where positiveness is guaranteed for sufficiently large  $\alpha_n$ ,  $\Sigma^0$  denotes the set of interior nodes of  $\Sigma$ ,  $\{ \{ \{ \{ \cdot \} \} \}_n$  and  $\{ \{ \cdot \} \}_n$  denotes the jump and the average at a node  $n$  of the values on neighboring segments. The matrix  $K_\Sigma$  comes from the discretization of  $-\partial_\tau^2$  using a symmetric interior penalty approach [3].

The DG discretization of (4.20) is then

$$(4.21) \quad \begin{aligned} (K_\Sigma + \alpha_1 M_\Sigma)(\Lambda_{2,\Omega_1} - \Lambda_2) &= (-K_\Sigma - i\tilde{\omega}\tilde{\sigma} M_\Sigma)(\Lambda_{1,\Omega_2} - \Lambda_1), \\ (K_\Sigma + \alpha_2 M_\Sigma)(\Lambda_{1,\Omega_2} - \Lambda_1) &= (-K_\Sigma - i\tilde{\omega}\tilde{\sigma} M_\Sigma)(\Lambda_{2,\Omega_1} - \Lambda_2), \end{aligned}$$

with  $\alpha_j = -2\tilde{\omega}^2 + i(\tilde{\omega}\tilde{\sigma} + 2\tilde{\omega}s_j)$ . As in the three-dimensional case,  $K_\Sigma$  is symmetric and non-negative definite, and  $M_\Sigma$  is symmetric and positive definite. A similar result to Theorem 4.1 can be obtained also in 2D:

**THEOREM 4.2** (DG discretization for the second-order conditions in 2D). *If  $s_1$  and  $s_2$  are such that  $s_j = p_j(1 + i)$  with  $p_j$  a strictly positive real number for  $j = 1, 2$ , then the relations (4.18) and (4.21) are equivalent.*

*Proof.* We first note that  $\Im \alpha_j = \tilde{\omega}\tilde{\sigma} + 2\tilde{\omega}p_j > 0$ . Setting

$$\mathbf{U}_1 = \Lambda_{1,\Omega_2} - \Lambda_1, \quad \mathbf{U}_2 = \Lambda_{2,\Omega_1} - \Lambda_2,$$

and multiplying the first relation in (4.21) on the left by  $\bar{\mathbf{U}}_2^T$ , the second by  $\bar{\mathbf{U}}_1^T$ , and adding them up, we obtain by taking the imaginary part

$$(\tilde{\omega}\tilde{\sigma} + 2\tilde{\omega}p_j)(\bar{\mathbf{U}}_1^T M_\Sigma \mathbf{U}_1 + \bar{\mathbf{U}}_2^T M_\Sigma \mathbf{U}_2) = -\tilde{\omega}\tilde{\sigma}(\bar{\mathbf{U}}_2^T M_\Sigma \mathbf{U}_1 + \bar{\mathbf{U}}_1^T M_\Sigma \mathbf{U}_2).$$

By rearranging the terms using the norm, we get

$$2\tilde{\omega}p_j(\|\mathbf{U}_1\|_{M_\Sigma}^2 + \|\mathbf{U}_2\|_{M_\Sigma}^2) + \tilde{\omega}\tilde{\sigma}\|\mathbf{U}_1 + \mathbf{U}_2\|_{M_\Sigma}^2 = 0.$$

From this last equation, we see that  $\mathbf{U}_j = 0$  since all the terms are positive, which proves the equivalence between (4.21) and (4.18).  $\square$

**5. Numerical results.** We illustrate the performance of the optimized Schwarz algorithms discretized using a DG method in two dimensions. We consider the TM formulation of Maxwell's equations, i.e.,  $\mathbf{E} = (0, 0, E_z)^T$  and  $\mathbf{H} = (H_x, H_y, 0)^T$ . We can then rewrite the algorithm in (3.1) by using that  $\mathbf{W} = (E_z, H_x, H_y)^T$  and the corresponding  $G$ -matrices are

$$G_0 = \begin{bmatrix} \tilde{\sigma} + i\tilde{\omega} & 0_{1 \times 2} \\ 0_{2 \times 1} & i\tilde{\omega}\mathbb{I}_{2 \times 2} \end{bmatrix}, \quad G_x = \begin{bmatrix} 0 & N_{\mathbf{e}_x} \\ N_{\mathbf{e}_x}^T & 0 \end{bmatrix}, \quad G_y = \begin{bmatrix} 0 & N_{\mathbf{e}_y} \\ N_{\mathbf{e}_y}^T & 0 \end{bmatrix},$$

TABLE 5.1  
*Symbols of the different operators for 2D Maxwell's equations.*

Algorithm	$\mathcal{F}(\tilde{S}_j)$
1	0
2	$-\frac{s-i\tilde{\omega}}{s+i\tilde{\omega}}, \quad s \in \mathbb{C}$
3	$-\frac{k^2+i\tilde{\omega}\tilde{\sigma}}{k^2-2\tilde{\omega}^2+i\tilde{\omega}\tilde{\sigma}+2i\tilde{\omega}s}, \quad s \in \mathbb{C}$
4	$-\frac{s_j-i\tilde{\omega}}{s_j+i\tilde{\omega}}, \quad s_j \in \mathbb{C}$
5	$-\frac{k^2+i\tilde{\omega}\tilde{\sigma}}{k^2-2\tilde{\omega}^2+i\tilde{\omega}\tilde{\sigma}+2i\tilde{\omega}s_j}, \quad s_j \in \mathbb{C}$

TABLE 5.2  
*Asymptotic convergence factor and optimal choice of the parameters in the transmission conditions for 2D Maxwell's equations.*

Algorithm	$\rho$	without overlap parameters
1	$1 - \frac{\tilde{\omega}^2 \tilde{\sigma}}{C^3} h^3$	none
2	$1 - \frac{2^{\frac{3}{4}} (\tilde{\omega} \tilde{\sigma})^{\frac{1}{4}} \sqrt{h}}{\sqrt{C}}$	$p = \frac{(\tilde{\omega} \tilde{\sigma})^{\frac{1}{4}} \sqrt{C}}{2^{\frac{1}{4}} \sqrt{h}}$
3	$1 - \frac{2^{\frac{11}{7}} (\tilde{\omega}^4 \tilde{\sigma}^2)^{\frac{1}{14}} h^{\frac{3}{7}}}{3^{\frac{3}{7}} C^{\frac{3}{7}}}$	$p = \frac{2^{\frac{4}{7}} (\tilde{\omega}^4 \tilde{\sigma}^2)^{\frac{1}{14}} C^{\frac{4}{7}}}{3^{\frac{3}{7}} h^{\frac{4}{7}}}$
4	$1 - \frac{(2 \tilde{\omega} \tilde{\sigma})^{\frac{1}{8}} h^{\frac{1}{4}}}{C^{\frac{1}{4}}}$	$p_1 = \frac{(2 \tilde{\omega} \tilde{\sigma})^{\frac{1}{8}} C^{\frac{3}{4}}}{h^{\frac{3}{4}}}, p_2 = \frac{(2 \tilde{\omega} \tilde{\sigma})^{3/8} C^{1/4}}{2 h^{\frac{1}{4}}}$
5	$1 - \frac{2^{\frac{34}{13}} (\tilde{\omega}^4 \tilde{\sigma}^2)^{\frac{1}{26}} h^{\frac{3}{13}}}{3^{\frac{3}{13}} C^{\frac{3}{13}}}$	$p_1 = \frac{2^{\frac{8}{13}} (\tilde{\omega}^4 \tilde{\sigma}^2)^{\frac{1}{26}} C^{\frac{10}{13}}}{3^{\frac{3}{13}} h^{\frac{10}{13}}}, p_2 = \frac{2^{\frac{11}{13}} (\tilde{\omega}^4 \tilde{\sigma}^2)^{\frac{3}{26}} C^{\frac{4}{13}}}{3^{\frac{9}{13}} h^{\frac{4}{13}}}$

where  $N_{\mathbf{n}} = (n_y, -n_x)^T$ . We present in Table 5.1 the corresponding Fourier symbols of  $\tilde{S}_j$  in the two-dimensional case, which were derived from the 3D results given in [16]. The parameters  $s = p(1+i)$ ,  $s_1 = p_1(1+i)$ , and  $s_2 = p_2(1+i)$  are solutions of specific min-max problems solved in [16], and their asymptotic behavior in the homogeneous non-overlapping case is displayed in Table 5.2 together with the corresponding convergence factors. The constant  $C$  is defined such that  $k_{\max} = \frac{C}{h}$  is the highest numerical frequency that can be represented by the discretization method on a mesh with mesh size  $h$ .

The Fourier symbols of the operators in Algorithms 1, 2, and 4 are constants, therefore their expression is the same in the physical space. In this case, (3.8) can be written in the 2D situation considered here as

$$(5.1) \quad \begin{aligned} E_1^{n+1} - N_{\mathbf{n}} \mathbf{H}_1^{n+1} + \tilde{S}_1(E_1^{n+1} + N_{\mathbf{n}} \mathbf{H}_1^{n+1}) &= E_2^n - N_{\mathbf{n}} \mathbf{H}_2^n + \tilde{S}_1(E_2^n + N_{\mathbf{n}} \mathbf{H}_2^n), \\ E_2^{n+1} + N_{\mathbf{n}} \mathbf{H}_2^{n+1} + \tilde{S}_2(E_2^{n+1} - N_{\mathbf{n}} \mathbf{H}_2^{n+1}) &= E_1^n + N_{\mathbf{n}} \mathbf{H}_1^n + \tilde{S}_2(E_1^n - N_{\mathbf{n}} \mathbf{H}_1^n). \end{aligned}$$

This is not the case for Algorithms 3 and 5, which lead to second-order transmission conditions because a factor of  $k^2$  appears in the corresponding Fourier symbols. As in the 3D case, we need to rewrite the transmission conditions: the  $\tilde{S}_j$  are operators with Fourier symbols

$$\mathcal{F}(\tilde{S}_j) = \frac{q_j(k)}{r_j(k)} \quad \text{with} \quad q_j(k) = -(k^2 + i\tilde{\omega}\tilde{\sigma}), \quad r_j(k) = k^2 - 2\tilde{\omega}^2 + i\tilde{\omega}\tilde{\sigma} + 2i\tilde{\omega}s_j.$$

We observe that the numerator and denominator,  $\mathcal{F}^{-1}(q_j)$  and  $\mathcal{F}^{-1}(r_j)$ , are partial differential

operators in the tangential direction,

$$\mathcal{F}^{-1}q_j = \partial_{\tau\tau} - i\tilde{\omega}\tilde{\sigma}, \quad \mathcal{F}^{-1}r_j = -\partial_{\tau\tau} - 2\tilde{\omega}^2 + i\tilde{\omega}\tilde{\sigma} + 2i\tilde{\omega}s_j.$$

In this case, we multiply the transmission conditions on both sides by the denominator, and then the interface iteration (5.1) can be rewritten as

$$\begin{aligned} \mathcal{F}^{-1}r_1(E_1^{n+1} - N_{\mathbf{n}}\mathbf{H}_1^{n+1}) + \mathcal{F}^{-1}q_1(E_1^{n+1} + N_{\mathbf{n}}\mathbf{H}_1^{n+1}) \\ = \mathcal{F}^{-1}r_1(E_2^n - N_{\mathbf{n}}\mathbf{H}_2^n) + \mathcal{F}^{-1}q_1(E_2^n + N_{\mathbf{n}}\mathbf{H}_2^n), \\ \mathcal{F}^{-1}r_2(E_2^{n+1} + N_{\mathbf{n}}\mathbf{H}_2^{n+1}) + \mathcal{F}^{-1}q_2(E_2^{n+1} - N_{\mathbf{n}}\mathbf{H}_2^{n+1}) \\ = \mathcal{F}^{-1}r_2(E_1^n + N_{\mathbf{n}}\mathbf{H}_1^n) + \mathcal{F}^{-1}q_2(E_1^n - N_{\mathbf{n}}\mathbf{H}_1^n), \end{aligned}$$

similarly to the general 3D case as we explained in (4.11).

**5.1. Plane wave in a homogeneous conductive medium.** We first consider the propagation of a plane wave in a homogeneous conductive medium. The computational domain is  $\Omega = (0, 1)^2$ , and  $\tilde{\sigma} = 0.5$ . We use DG discretizations with several polynomial orders denoted by  $\text{DG-}\mathbb{P}_k$ , with  $k = 1, 2, 3, 4$ , and impose on  $\partial\Omega = \Gamma_a$  an incident wave

$$\mathbf{W}_{\text{inc}} = \begin{bmatrix} \frac{k_y}{\tilde{\omega}} \\ -\frac{k_x}{\tilde{\omega}} \\ 1 \end{bmatrix} e^{-i\mathbf{k}\cdot\mathbf{x}}, \quad \text{and} \quad \mathbf{k} = \begin{bmatrix} k_x \\ k_y \end{bmatrix} = \begin{bmatrix} \tilde{\omega}\sqrt{1 - i\frac{\tilde{\sigma}}{\tilde{\omega}}} \\ 0 \end{bmatrix}.$$

The domain  $\Omega$  is decomposed into the two subdomains  $\Omega_1 = (0, 0.5) \times (0, 1)$  and  $\Omega_2 = (0.5, 1) \times (0, 1)$ . The goal of this first test problem is to retrieve numerically the asymptotic behavior of the convergence factors of the optimized Schwarz methods when discretized using DG and to compare with the theoretical convergence factors of Table 5.2. The iteration numbers to reduce the relative residual by six orders of magnitude are given in Table 5.3, where also in parentheses the iteration numbers are included for the use of the Schwarz methods as preconditioners for a Krylov method, which is BiCGStab in our case. We clearly see that there is a hierarchy of faster and faster algorithms, and their asymptotic behavior corresponds well to the analysis as one can see from Figure 5.1.

**5.2. Plane wave in a multi-layer heterogeneous medium.** We study the performance of the optimized Schwarz algorithms in the case of a heterogeneous propagation medium. The model problem we consider is the propagation of a plane wave in a multi-layer conductive medium, as displayed in Figure 5.2 on the left. We decompose the computational domain  $\Omega = (-1, 1)^2$  into two subdomains  $\Omega_1 = (0, 0.5) \times (0, 1)$  and  $\Omega_2 = (0.5, 1) \times (0, 1)$ ; see Figure 5.2 on the right. The electromagnetic characteristics of the medium are given in Table 5.4.

We test here the method  $\text{DG-}\mathbb{P}_{1,2,3,4}$  where the interpolation degree is fixed for each element of the mesh according to the local wavelength; see the last column in Table 5.4. In Table 5.5, we again present the iteration numbers obtained by the various optimized Schwarz algorithms for reducing the relative residual by six orders of magnitude and in parentheses the corresponding iteration numbers when the Schwarz methods are used as preconditioners. In Figure 5.3, we plot these iteration numbers as a function of the mesh size as well as the corresponding theoretical asymptotic iteration number counts, which shows that even in such a layered medium, where our analysis is not valid any more, the Schwarz algorithms still behave asymptotically as the constant medium theory indicates. We finally display in 5.4 the real part of the electric field for this scattering problem.

TABLE 5.3

*Wave propagation in a homogeneous medium. Iteration count as a function of  $h$  when the optimized Schwarz methods are used as iterative solvers and in parentheses when used as preconditioners.*

	$h$			
	$\frac{1}{10}$	$\frac{1}{20}$	$\frac{1}{40}$	$\frac{1}{80}$
	DG- $\mathbb{P}_1, \tilde{\omega} = 2\pi$			
Algorithm 1	383 (16)	1396 (21)	5434 (27)	24400 (35)
Algorithm 2	30 (9)	43 (11)	62 (13)	92 (18)
Algorithm 3	29 (9)	40 (10)	59 (13)	81 (18)
Algorithm 4	28 (10)	34 (10)	43 (12)	52 (17)
Algorithm 5	28 (9)	32 (9)	38 (10)	45 (15)
	DG- $\mathbb{P}_2, \tilde{\omega} = 10/3\pi$			
Algorithm 1	1573 (21)	2288 (24)	10520 (29)	55054 (35)
Algorithm 2	37 (11)	53 (12)	77 (16)	111 (18)
Algorithm 3	35 (10)	48(11)	69 (16)	95 (17)
Algorithm 4	30 (10)	36 (12)	45 (14)	55 (16)
Algorithm 5	29 (9)	33 (10)	39 (13)	49 (14)
	DG- $\mathbb{P}_3, \tilde{\omega} = 13/3\pi$			
Algorithm 1	650 (21)	3025 (25)	17900 (30)	(51)
Algorithm 2	40 (11)	58 (14)	84 (16)	122 (21)
Algorithm 3	38 (11)	51 (13)	75 (15)	105 (19)
Algorithm 4	31 (10)	38 (13)	47 (15)	57 (19)
Algorithm 5	30 (9)	33 (11)	39 (13)	47 (16)
	DG- $\mathbb{P}_4, \tilde{\omega} = 6\pi$			
Algorithm 1	1072 (29)	6318 (38)	39977 (51)	(64)
Algorithm 2	50 (12)	73 (15)	106 (18)	154 (21)
Algorithm 3	47 (11)	69 (14)	98 (18)	139 (20)
Algorithm 4	37 (12)	47 (14)	59 (17)	71 (19)
Algorithm 5	34 (10)	42 (12)	51 (15)	60 (17)

TABLE 5.4

*Characteristic parameters of the medium for the model problem of scattering of a plane wave in a multi-layer domain.*

Layer $i$	$\varepsilon_i$	$\tilde{\sigma}_i$	$\mu_i$	DG- $\mathbb{P}_i$
1	1.0	0.0	1	1
2	2.25	0.1	1	2
3	3.5	0.2	1	3
4	5.3	0.5	1	4

**5.3. Scattering of a plane wave by a conductive dielectric cylinder.** The final model problem we consider is the scattering of a plane wave by a dielectric conductive cylinder with radius  $r_0 = 0.6$  m. The computational domain is obtained by artificially restricting the domain to a cylinder with radius  $r = 1.6$  m and using the Silver-Müller condition on the artificial boundary. We use a non-uniform triangular mesh which consists of 2078 vertices and 3958 triangles; see Figure 5.5. The relative permittivity of the inner cylinder is set to  $\varepsilon_r = 2.25$  and its electric conductivity to  $\tilde{\sigma} = 0.01$ , while vacuum is assumed for the rest of the domain. The frequency we consider is  $F=300$  MHz. Numerical simulations are performed



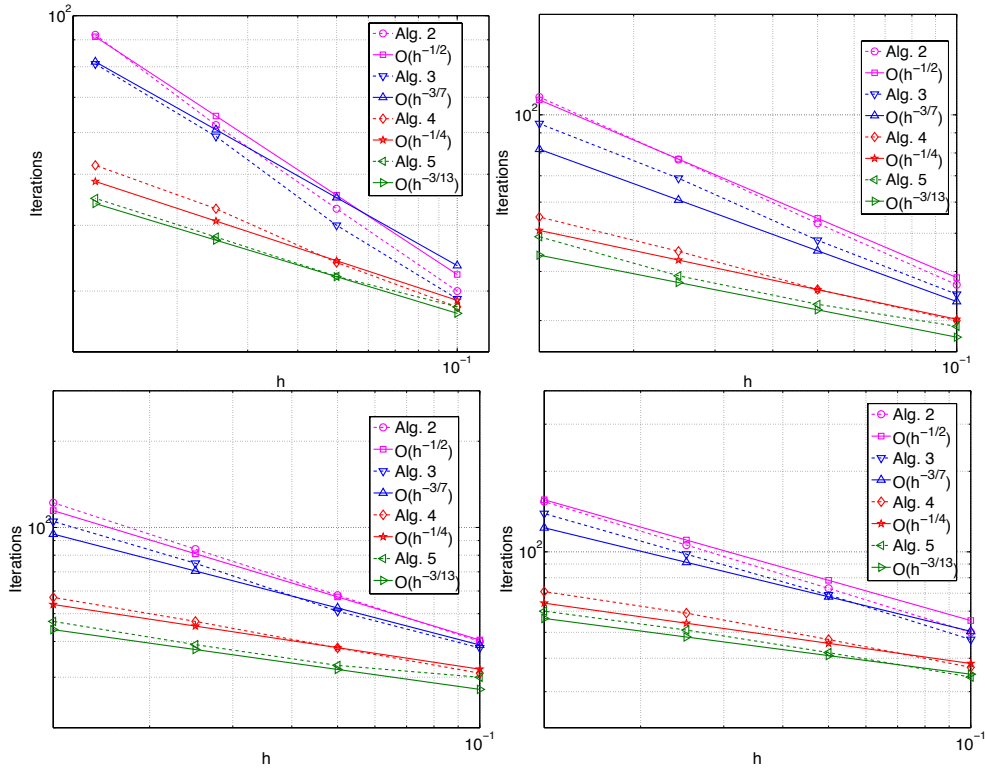


FIG. 5.1. Asymptotic behavior of the iteration numbers from Table 5.3 as a function of the mesh size  $h$  for the  $DG-P_1$ ,  $DG-P_2$ ,  $DG-P_3$ , and  $DG-P_4$  discretizations.

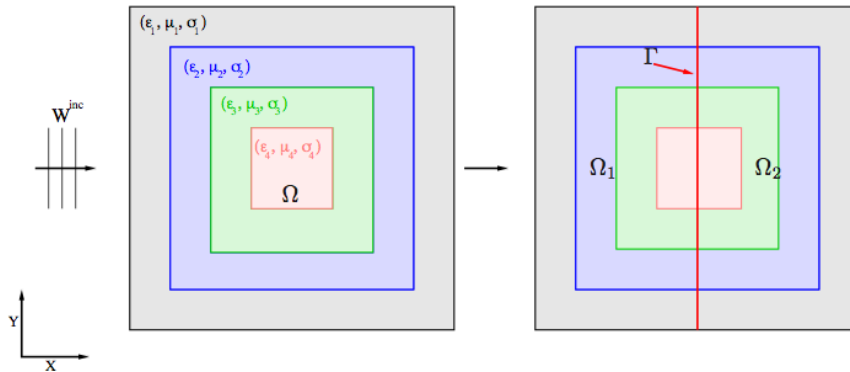


FIG. 5.2. Domain configuration for the model problem of scattering of a plane wave in a multi-layer domain.

using decompositions into 4 and 16 subdomains; for an example see Figure 5.5. In Table 5.6 we display the iteration numbers for the various optimized Schwarz methods for reducing the relative residual by six orders of magnitude. Here,  $DG-P_{1,2,3,4}$  stands for a non-uniform-order DG discretization, i.e., the interpolation order is defined on an elementwise basis: small elements use low-order shape functions and large elements use high-order ones. We note that the optimized algorithms improve substantially the convergence of the classical Schwarz

TABLE 5.5

*Scattering of a plane wave in a multi-layer domain. Iteration count as a function of  $h$  when the optimized Schwarz methods are used as iterative solvers and in parentheses when used as preconditioners.*

	$h$			
	$\frac{1}{20}$	$\frac{1}{40}$	$\frac{1}{80}$	$\frac{1}{160}$
Algorithm 1	727 (31)	2974 (41)	11973 (52)	(70)
Algorithm 2	108 (21)	153(25)	220 (30)	315 (33)
Algorithm 3	101 (20)	138 (23)	197 (27)	267 (30)
Algorithm 4	87 (18)	103 (22)	128 (25)	157 (28)
Algorithm 5	84 (16)	96 (20)	113 (22)	140 (25)

TABLE 5.6

*Scattering of a plane wave by a dielectric conductive cylinder. Iteration count vs. mesh size.*

Algo.	DG- $\mathbb{P}_1$		DG- $\mathbb{P}_2$		DG- $\mathbb{P}_3$		DG- $\mathbb{P}_4$		DG- $\mathbb{P}_{1,2,3,4}$	
	# of domains		# of domains		# of domains		# of domains		# of domains	
	4	16	4	16	4	16	4	16	4	16
1	76	104	99	145	124	168	134	203	78	105
2	33	50	40	62	50	66	52	81	34	51
3	32	47	38	57	46	62	48	75	31	48
4	29	45	36	53	44	58	42	70	29	46
5	28	42	33	50	40	55	39	76	28	44

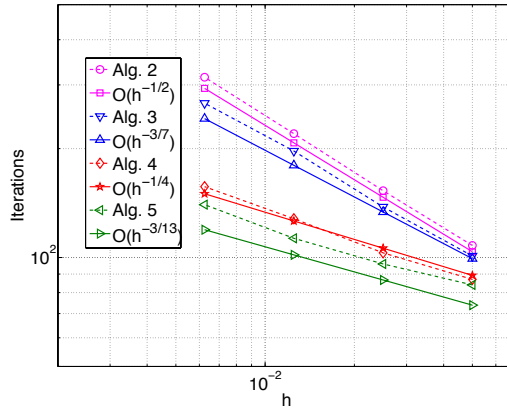


FIG. 5.3. Asymptotic behavior of the iteration numbers from Table 5.5 as a function of the mesh size  $h$ .

algorithm (Algorithm 1 in the table) and also that the gain between both the optimized and the classical algorithms seems to slightly increase with the interpolation order. Finally, we also observe, as could be expected, a dependence of the iteration count on the number of subdomains since we are not using any coarse grid correction in these experiments.

**6. Conclusions.** In this paper we have shown how optimized Schwarz methods can be properly discretized in the framework of DG-methods such that at convergence, the result of the underlying DG monodomain solution is recovered. The key idea is to introduce additional trace variables on each subdomain interface representing the DG-traces of the neighboring subdomain interface traces and then to use both traces appropriately to discretize the optimized transmission conditions. We have tested the performance of the DG-discretized Schwarz

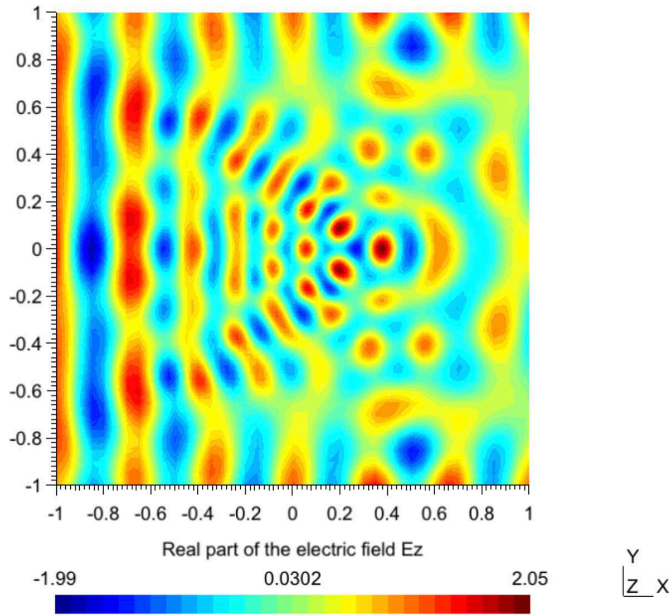


FIG. 5.4. *Real part of the electric field for the scattering of a plane wave in a multi-layer domain.*

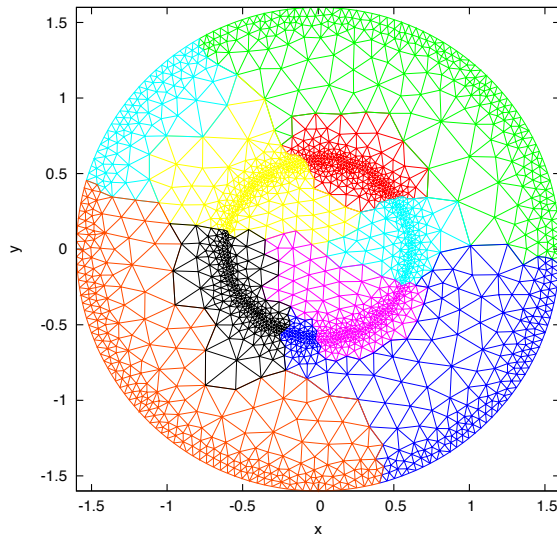


FIG. 5.5. *Mesh and subdomain decomposition for the scattering problem of a plane wave by a dielectric conductive cylinder.*

methods on many numerical scattering experiments, both for homogeneous and heterogeneous media and in various physical configurations and for various decompositions. Our numerical results indicate that the asymptotic performance of these algorithms obtained at a theoretical level for homogeneous media and constant coefficients well predicts the performance of the algorithms when discretized using DG-discretizations, both in homogeneous and heterogeneous media and for very general decompositions.

## REFERENCES

- [1] A. ALONSO RODRÍGUEZ AND L. GERARDO-GIORDA, *New nonoverlapping domain decomposition methods for the harmonic Maxwell system*, SIAM J. Sci. Comput., 28 (2006), pp. 102–122.
- [2] D. N. ARNOLD, *An interior penalty finite element method with discontinuous elements*, SIAM J. Numer. Anal., 19 (1982), pp. 742–760.
- [3] D. N. ARNOLD, F. BREZZI, B. COCKBURN, AND L. D. MARINI, *Unified analysis of discontinuous Galerkin methods for elliptic problems*, SIAM J. Numer. Anal., 39 (2001/02), pp. 1749–1779.
- [4] A. BUFFA, M. COSTABEL, AND D. SHEEN, *On traces for  $H(\text{curl}, \Omega)$  in Lipschitz domains*, J. Math. Anal. Appl., 276 (2002), pp. 845–867.
- [5] A. BUFFA AND I. PERUGIA, *Discontinuous Galerkin approximation of the Maxwell eigenproblem*, SIAM J. Numer. Anal., 44 (2006), pp. 2198–2226.
- [6] P. CHEVALIER AND F. NATAF, *Symmetrized method with optimized second-order conditions for the Helmholtz equation*, in Domain Decomposition Methods 10: The 10th International Conference on Domain Decomposition Methods, Boulder, 1997, J. Mandel, C. Farhat, and X.-C. Cai, eds., Contemp. Math., 218, Amer. Math. Soc., Providence, 1997, pp. 400–407.
- [7] P. COLLINO, G. DELBUE, P. JOLY, AND A. PIACENTINI, *A new interface condition in the non-overlapping domain decomposition for the Maxwell equations*, Comput. Methods Appl. Mech. Engrg., 148 (1997), pp. 195–207.
- [8] B. DESPRÉS, *Décomposition de domaine et problème de Helmholtz*, C. R. Acad. Sci. Paris Sér. I Math., 311 (1990), pp. 313–316.
- [9] B. DESPRÉS, P. JOLY, AND J. E. ROBERTS, *A domain decomposition method for the harmonic Maxwell equations*, in Iterative Methods in Linear Algebra, Proceedings of the IMACS International Symposium held at the Vrije Universiteit Brussel, 1991, R. Beauwens and P. de Groen, eds., North-Holland, Amsterdam, 1992, pp. 475–484.
- [10] V. DOLEAN, H. FOL, S. LANTERI, AND R. PERRUSSEL, *Solution of the time-harmonic Maxwell equations using discontinuous Galerkin methods*, J. Comput. Appl. Math., 218 (2008), pp. 435–445.
- [11] V. DOLEAN, M. J. GANDER, AND L. GERARDO-GIORDA, *Optimized Schwarz methods for Maxwell's equations*, SIAM J. Sci. Comput., 31 (2009), pp. 2193–2213.
- [12] V. DOLEAN, M. J. GANDER, S. LANTERI, J.-F. LEE, AND Z. PENG, *Optimized Schwarz methods for curl-curl time-harmonic Maxwell's equations*, in Domain Decomposition Methods in Science and Engineering 21, J. Erhel, M. J. Gander, L. Halpern, T. Sassi, and O. Widlund, eds., Lect. Notes Comput. Sci. Eng., 98, Springer, Cham, 2014, pp. 587–595.
- [13] ———, *Effective transmission conditions for domain decomposition methods applied to the time-harmonic curl-curl Maxwell's equations*, J. Comput. Phys., 280 (2015), pp. 232–247.
- [14] V. DOLEAN, S. LANTERI, AND R. PERRUSSEL, *A domain decomposition method for solving the three-dimensional time-harmonic Maxwell equations discretized by discontinuous Galerkin methods*, J. Comput. Phys., 227 (2008), pp. 2044–2072.
- [15] ———, *Optimized Schwarz algorithms for solving time-harmonic Maxwell's equations discretized by a discontinuous Galerkin method*, IEEE. Trans. Magnetics, 44 (2008), pp. 954–957.
- [16] M. EL BOUJAJI, V. DOLEAN, M. J. GANDER, AND S. LANTERI, *Optimized Schwarz methods for the time-harmonic Maxwell equations with damping*, SIAM J. Sci. Comput., 34 (2012), pp. A2048–A2071.
- [17] M. EL BOUJAJI, V. DOLEAN, M. J. GANDER, S. LANTERI, AND R. PERRUSSEL, *DG discretization of optimized Schwarz methods for Maxwell's equations*, in Domain Decomposition Methods in Science and Engineering 21, J. Erhel, M. J. Gander, L. Halpern, T. Sassi, and O. Widlund, eds., Lect. Notes Comput. Sci. Eng., 98, Springer, Cham, 2014, pp. 217–225.
- [18] O. G. ERNST AND M. J. GANDER, *Why it is difficult to solve Helmholtz problems with classical iterative methods*, in Numerical Analysis of Multiscale Problems, I. G. Graham, T. Y. Hou, O. Lakkis, and R. Scheichl, eds., Lect. Notes Comput. Sci. Eng., 83, Springer, Heidelberg, 2012, pp. 325–363.
- [19] M. J. GANDER, *Optimized Schwarz methods*, SIAM J. Numer. Anal., 44 (2006), pp. 699–731.
- [20] ———, *Schwarz methods over the course of time*, Electron. Trans. Numer. Anal., 31 (2008), pp. 228–255. <http://etna.math.kent.edu/vol.31.2008/pp228-255.dir>
- [21] M. J. GANDER AND S. HAJIAN, *Block Jacobi for discontinuous Galerkin discretizations: no ordinary Schwarz methods*, in Domain Decomposition Methods in Science and Engineering 21, J. Erhel, M. J. Gander, L. Halpern, T. Sassi, and O. Widlund, eds., Lect. Notes Comput. Sci. Eng., 98, Springer, Cham, 2014, pp. 305–313.
- [22] ———, *Analysis of Schwarz methods for a hybridizable discontinuous Galerkin discretization*, SIAM J. Numer. Anal., 53 (2015), pp. 573–597.
- [23] M. J. GANDER, F. MAGOULÈS, AND F. NATAF, *Optimized Schwarz methods without overlap for the Helmholtz equation*, SIAM J. Sci. Comput., 24 (2002), pp. 38–60.
- [24] S. HAJIAN, *An optimized Schwarz algorithm for discontinuous Galerkin methods*, in Domain Decomposition Methods in Science and Engineering 22, T. Dickopf, M. J. Gander, L. Halpern, R. Krause, and

- L. F. Pavarino, eds., Lect. Notes Comput. Sci. Eng., 104, Springer, Cham, 2015, to appear.
- [25] P. HELLUY, *Résolution numérique des équations de Maxwell harmoniques par une méthode d'éléments finis discontinus*, Ph.D. Thesis, Mathématiques Appliquées, Ecole Nationale Supérieure de l'Aéronautique et de l'espace, Toulouse, 1994.
- [26] P. HELLUY AND S. DAYMA, *Convergence d'une approximation discontinue des systèmes du premier ordre*, C. R. Acad. Sci. Paris Sér. I Math., 319 (1994), pp. 1331–1335.
- [27] P. HELLUY, P. MAZET, AND P. KLOTZ, *Sur une approximation en domaine non borné des équations de Maxwell instationnaires: comportement asymptotique*, Rech. Aérospat., 5 (1994), pp. 365–377.
- [28] J. HESTHAVEN AND T. WARBURTON, *Nodal Discontinuous Galerkin methods: Algorithms, Analysis and Applications*, Springer, New York, 2008.
- [29] P. HOUSTON, I. PERUGIA, A. SCHNEEBELI, AND D. SCHÖTZAU, *Interior penalty method for the indefinite time-harmonic Maxwell equations*, Numer. Math., 100 (2005), pp. 485–518.
- [30] ———, *Mixed discontinuous Galerkin approximation of the Maxwell operator: the indefinite case*, M2AN Math. Model. Numer. Anal., 39 (2005), pp. 727–753.
- [31] S.-C. LEE, M. N. VOUVAKIS, AND J.-F. LEE, *A non-overlapping domain decomposition method with non-matching grids for modeling large finite antenna arrays*, J. Comput. Phys., 203 (2005), pp. 1–21.
- [32] Z. PENG AND J.-F. LEE, *Non-conformal domain decomposition method with second-order transmission conditions for time-harmonic electromagnetics*, J. Comput. Phys., 229 (2010), pp. 5615–5629.
- [33] ———, *A scalable nonoverlapping and nonconformal domain decomposition method for solving time-harmonic maxwell equations in  $\mathbb{R}^3$* , SIAM J. Sci. Comput., 34 (2012), pp. A1266–A1295.
- [34] Z. PENG, V. RAWAT, AND J.-F. LEE, *One way domain decomposition method with second order transmission conditions for solving electromagnetic wave problems*, J. Comput. Phys., 229 (2010), pp. 1181–1197.
- [35] I. PERUGIA, D. SCHÖTZAU, AND P. MONK, *Stabilized interior penalty methods for the time-harmonic Maxwell equations*, Comput. Methods Appl. Mech. Engrg., 191 (2002), pp. 4675–4697.
- [36] V. RAWAT, *Finite Element Domain Decomposition with Second Order Transmission Conditions for Time-Harmonic Electromagnetic Problems*, Ph.D. Thesis, ElectroScience Lab, Ohio State University, Columbus, 2009.
- [37] V. RAWAT AND J.-F. LEE, *Nonoverlapping domain decomposition with second order transmission condition for the time-harmonic Maxwell's equations*, SIAM J. Sci. Comput., 32 (2010), pp. 3584–3603.